British Geological Survey

Data discovery for Boulby Underground Laboratory and associated Zechstein deposits of NE England and Southern North Sea

Secure Underground Caverns as an Energy Storage Solution - SUCcESS

Open Report OR/24/051

BRITISH GEOLOGICAL SURVEY

Secure Underground Caverns as an Energy Storage Solution -SUCcESS

OPEN REPORT OR/24/051

Keywords

Energy Storage, Geomechanics, Hydrogen Storage, Boulby Underground Laboratory, Halite

Bibliographical reference

ARMITAGE T., HOUGH E., DAMASCHKE M., 2024. Data discovery for Boulby Underground Laboratory and associated Zechstein deposits of NE England and Southern North Sea. *British Geological Survey Internal Report*, OR/24/051. 41pp.

Data discovery for Boulby Underground Laboratory and associated Zechstein deposits of NE England and Southern North Sea

T. Armitage, E. Hough, Damaschke M.

Keyworth, Nottingham British Geological Survey 2024

BRITISH GEOLOGICAL SURVEY

The full range of our publications is available from BGS shops at Nottingham, Edinburgh, London and Cardiff (Welsh publications only) see contact details below or shop online at www.geologyshop.com

The London Information Office also maintains a reference collection of BGS publications, including maps, for consultation.

We publish an annual catalogue of our maps and other publications; this catalogue is available online or from any of the BGS shops.

The British Geological Survey carries out the geological survey of Great Britain and Northern Ireland (the latter as an agency service for the government of Northern Ireland), and of the surrounding continental shelf, as well as basic research projects. It also undertakes programmes of technical aid in geology in developing countries.

The British Geological Survey is a component body of UK Research and Innovation.

British Geological Survey offices

Nicker Hill, Keyworth,
Nottingham NG12 5GG
Tel 0115 936 3100

BGS Central Enquiries Desk
Tel 0115 936 3143
email enquiries@bgs.ac.uk

BGS Sales
Tel 0115 936 3241
email sales@bgs.ac.uk

The Lyell Centre, Research Avenue South,
Edinburgh EH14 4AP
Tel 0131 667 1000
email scotsales@bgs.ac.uk

Natural History Museum, Cromwell Road,
London SW7 5BD
Tel 020 7589 4090
Tel 020 7942 5344/45
email bgslondon@bgs.ac.uk

Cardiff University, Main Building, Park Place,
Cardiff CF10 3AT
Tel 029 2167 4280

Maclean Building, Crowmarsh Gifford,
Wallingford OX10 8BB
Tel 01491 838800

Geological Survey of Northern Ireland, 7th Floor,
Adelaide House, 39-49 Adelaide Street, Belfast, BT2 8FD
Tel 0289 038 8462
www2.bgs.ac.uk/gsni/

Natural Environment Research Council, Polaris House,
North Star Avenue, Swindon SN2 1EU
Tel 01793 411500 Fax 01793 411501
www.nerc.ac.uk

UK Research and Innovation, Polaris House,
Swindon SN2 1FL
Tel 01793 444000
www.ukri.org

Website www.bgs.ac.uk
Shop online at www.geologyshop.com

Contents

FIGURES

TABLES

Summary

This report summarises publicly available data related to Boulby Mine, Boulby Underground Laboratory (BUL) and their host geology of the Zechstein deposits of the Southern Permian Basin. The work completed was part of the Secure Underground Caverns as an Energy Storage Solution (SUCcESS) project, an STFC-funded venture to develop a research roadmap for geological research utilising the facilities and geology available at BUL.

The first section of the report introduces the project within the context for net zero, requirement for energy storage and the role of halite and BUL within geological research. Following this is an overview of the physical properties of halite, summary of the current understanding for the Zechstein Supergroup of NE England and offshore Southern North Sea, the local geology for Boulby, and publicly accessible data for the Boulby Halite. Concluding the report is a summary of relevant research into the geomechanical and thermodynamic responses to hydrogen storage within salt caverns, and research gaps that may be exploited using the resources available at Boulby Underground Laboratory.

1 Introduction and UK net zero context

The United Kingdom's energy mix will undergo a significant shift as it pivots aways from hydrocarbons to meet its 2050 net zero carbon target. One method of lowering carbon emissions is to reduce reliance on hydrocarbons and replace fossil fuel energy sources for low-carbon and renewable alternatives, such as wind, photovoltaic solar and nuclear power. The United Kingdom has access to an abundance of wind renewable energy, with government targets of 50 GW of offshore wind capacity by 2030 proving to be a key building block for the green energy transition to meet the United Kingdom's Paris Climate goal. However, as the reliance on hydrocarbons decreases and intermittent renewable energy penetration increases in the electricity and energy systems, balancing supply and demand will become increasingly difficult. To decarbonise and achieve the net zero emissions targets while also producing enough energy to provide for national energy needs, large-scale, low-carbon energy generation projects need to be developed alongside energy storage facilities to provide flexibility within a low carbon energy supply. Recent studies have estimated 66 TWh (Cárdenas *et al.* 2021a, b) of energy storage may be required to decarbonise the British electricity grid, *c.* 55 TWh of which would be hydrogen, while 100 TWh may be required to the United Kingdom to meet net zero by 2050 (Royal Society, 2023).

Currently, hydrocarbon energy storage holds by far the largest capacity in the United Kingdom, with 30 TWh of storage for methane in 2023 (National Grid ESO; Wilson 2023). This is distributed between the Rough gas field in the Southern North Sea, a key anchor of UK energy policy for >10 years, total storage in salt caverns and gas opening stock held as liquified natural gas. However, hydrogen is postulated as a natural replacement for methane in the UK energy system, allowing for decarbonisation of hard to ablate sectors such as industrial processes and transport, and for use as an energy vector and energy storage medium (Royal Society, 2023). At large scale (>0.5 TWh), hydrogen is thought to be most cheaply stored underground either in lined rock caverns, salt caverns or depleted gas fields (Lord et al., 2014). However, the lower energy density of hydrogen means that a greater storage volume will be required for hydrogen to meet the same energy stored as natural gas.

The Humber and Teesside industrial clusters are major centres of economic activity that host carbon-intensive sectors (Humberside Industrial Cluster Plan UKRI 2022; Tees Valley Combined Authority 2023; IDRIC 2024). Storing energy proximal to these key centres of energy-intensive industry is key for strategic energy planning. Salt caverns are one such technology that may be used to store energy, either as compressed air (CAES) or in the form of hydrogen. While hydrogen has been stored in salt caverns at Teesside since the 1970's, CAES is not commercially deployed in the UK and uncertainties remain over the economic feasibility along with technical upscaling of cavern capacity.

The subsurface geology of onshore NE England and the adjacent offshore region has the potential capacity to contribute significantly to fulfilling the UK's future low carbon energy demand, energy storage needs and carbon dioxide sequestration targets (Williams et al., 2022; Underhill *et al.,* 2023). Underlying this region is the Southern Permian Basin and Zechstein Supergroup. Historically, this region has been a significant energy producer for hydrocarbons since the 1960's with exploration of the Southern North Sea for natural gas, however, recently has become the target of carbon capture and storage and hydrogen storage investigations (Fyfe and Underhill 2023a). The area also crucially hosts the Boulby and Woodsmith mines (latter under development), which exploit large halite and polyhalite deposits hosted within the Zechstein Supergroup. Boulby also hosts the Boulby Underground Laboratory[1], a collaborative geophysical and physics laboratory that uses the subsurface conditions to investigate geo- and astro- physics (Daniels *et al.* 2023). Across this geological area, a wealth of understanding has been gathered on the Southern Permian Basin which may be exploited and critiqued using the latest geological literature. Therefore, a detailed literature review of the basin and supergroup is given, with particular emphasis on relevant Zechstein depositional cycles that may be used for

[1] https://www.boulby.stfc.ac.uk/Pages/home.aspx

energy storage in East England and the Boulby Mine exposures. After this, a review of the latest research for salt use in hydrogen storage is provided, gathered from a range of academic and grey literature, BGS georeport and Solution Mining Research Institute conference papers. Collectively, this data discovery exercise gives the state-of-the-art understanding of the latest relevant research at Boulby and identify research gaps that may be explored using BUL.

2 Overview of halite properties relating to salt caverns

Halite is the mineral name for rock salt, composed of sodium chloride (NaCl) and is classified as an evaporite. It is commonly precipitated as a chemical sediment in sedimentary basins from marine, continental, or mixed marine-continental brines that are supersaturated with respect to NaCl (Handford, 1991). Halite is often perceived as being of high-purity and colourless. However, most bedded halite-bearing strata, including those of the UK contain impurities, such as other evaporites or insoluble particles, such as clays or anhydrite.

Two basic structural formations of halite are recognised:

Bedded, which occur as massively bedded halite deposits, largely as they were immediately post-deposition (precipitation) and often retaining original crystal and sedimentological fabrics.

Domal, which are deposits that have undergone mobilisation (halokinesis), involving multiple phases of recrystallisation, to form large swells/pillows, diapirs and walls that deform and may breach overburden strata.

The structural formation of halite may greatly impact the lateral extent, thickness, heterogeneity, internal structure (e.g., the presence of entrained insoluble material or “stringers”), external contacts and deformation of surrounding strata, and internal crystallographic properties of the halite. Individual halite properties may also be site-specific and change on a basin and sub-basin scale (Warren, 2006, 2017). However, there are some structural and crystallographic characteristics that are shared between deposits which may be of interest.

Halite is almost incompressible to depths of 6-8 km, which often contrasts with overlying sedimentary strata that contracts, loses porosity and become denser and stronger than the underlying halite. This produces an effective buoyancy compared to other sedimentary strata after *c.* 1 km depth of burial (White et al., 2018). Few other rocks are as plastic as halite, which combined with the effective buoyancy produces salt migration or halokinesis. Halite viscosity typically ranges from 1013 to 1016 Pa s^{-1} (White et al., 2018). Halite is also highly thermally conductive, (at 43 ^{o}C, the thermal conductivity of halite is 5.13 W/m-K; Warren, 2006), which can be three-times higher than surrounding sediments. Meanwhile, the unconfined compressive strength is between 12 and 25 MPa, with an average of 20 MPa (Hansen et al., 2016). Halite has a low tensile strength with values ranging 0.5-1.5 MPa, with similar uniaxial tensile strength between bedded and domal (Hansen et al., 2016).

Halite deforms via crystal plastic deformation (recrystallisation) processes including dislocation creep (combinations of slip, glide or dislocation), diffusive creep (Coble creep), or crystal lattice (Nabarro-Herring creep), pressure solution or grain boundary migration. Deforming halite has negligible shear strength on geological time scales, behaving as a pseudo fluid, with thick beds acting as a pressurised, ductile layer and effectively representing a lubricant that decouples the overburden from the basement. These characteristics allow for some degree of self-seal/heal damage which occurs over different spatial and temporal scales leading to recrystallisation and changes to halite fabrics at the small scale and to salt tectonics or halokinesis at larger scales (Swift and Reddish 2005).

Salt creep rates increase exponentially with a linear increase in temperature; thus, although thermal effects may need to be accounted for at all levels, they are most significant at greater depths or in areas of elevated geothermal gradient. An elastic-plastic transition zone will occur roughly at 1 km depth, after which salt will deform (creep) at faster rates. Salt creep is also accelerated by large differences between natural lithostatic pressure and the internal gas pressure of the cavern. Specific creep rates, and depths at which they occur, are dependent upon the composition, proportions and physical properties of the various salt minerals and non-halite lithologies.

The dominant deformation mechanism for halite is visco-plastic, i.e. creep. However, when strain rate exceeds the ductile deformation accommodation rate, brittle deformation may be observed. In nature, this is expressed as fractures and faulting and may be the result of

anthropogenic activity like mine blasting or convergence near human-made voids (White et al., 2018). Over geological time and under suitable temperature and pressure conditions, halite that has undergone brittle deformation will anneal.

Most evaporites form highly efficient seals to gas and fluids as an impermeable rock, with zero transmissivity maintained over geological periods (tens of millions of years; Warren, 2006; 2017). Typically, bedded evaporite successions, especially beds of predominantly monomineralic composition (e.g. massive halite/rock salt), have entry pressures greater than 20.6 MPa (206 bar/3000 psi), with impure evaporite beds having entry pressures greater than 6.9 MPa (69 bar/1000 psi). These entry pressures contrast with those for most shales (which are water-bearing) of 6.2–6.9 MPa (900-1000 psi) (Warren, 2006) but may be 10 MPa or more in some fully saturated shales (e.g. Marschall et al., 2005). In the context for gaseous storage, it may be argued that pure unfractured halite and evaporitic sequences are impermeable on the storage timescales required, although repeated damage and healing over short timescales require further investigations.

Due to its favourable deformation characteristics, low permeability, high solubility and low reactivity, salt has been solution mined to create caverns in the subsurface for decades which have been used to store liquid or gaseous products for the chemicals industries, such as hydrogen, or compressed air such as Huntdorf in Germany (Kaldemeyer et al., 2016). However, such caverns require careful management and operational planning to maintain cavern integrity and minimise leakage.

The depth, and thus temperature and lithostatic pressure, of the cavern is therefore highly impacts the creep rate and longevity of the cavern. For example, caverns at Eminence, constructed at 1.7-2 km depth, lost up to 40% of their volume in just two years post construction (Allen, 1972). Here, caverns were operated down to atmospheric pressure for significant periods of time and volume losses were stopped with the implementation of minimum gas pressures during storage operations. This shows the importance of careful design, construction and operational management of internal pressure. Under careful management, a cavern volume loss of a couple of percent per year may otherwise be expected (Warren, 2006).

3 Salt Caverns for hydrogen storage in the UK

Underground salt cavern storage has been employed as a geological storage technology for decades and offers the potential to store hydrogen in large volumes (GWh) at a comparable or cheaper price to surface tanks (Ahluwalia *et al.* 2019; Lord *et al.* 2014; James *et al.* 2016; Miocic *et al.* 2023). Solution-mined caverns in salt structures are already in widespread use as subsurface energy storage facilities for natural gas onshore in many parts of the world, and as hydrogen storage onshore in the UK and US (Miocic *et al.* 2023). The physical and chemical properties of salt are beneficial to hydrogen storage as salt is chemically inert with respect to hydrogen, has an ability to endure cyclic loading storage operations through 'sealing/annealing' (dynamic creep), and has a low porosity and permeability to hydrogen. Salt may easily be dissolved and engineered caverns constructed, with salt by-product sometimes used for chemical processes. Finally, the storage volume and boundary conditions of salt cavern can be more easily managed than porous media storage, allowing for fast cycling and a reduced volume of cushion gas needed.

Currently, only a few sites exist for hydrogen storage (>95% hydrogen) in salt caverns, located at Teesside (UK), and Clemens Dome, Spindletop and Moss Bluff (USA) (Tarkowski 2019). Teesside has been storing hydrogen since 1970 in three elliptical shaped caverns at a depth of 350-400 m within the Zechstein Supergroup with a total volume of 210,000 m^3 (Caglayan *et al.* 2020; Williams *et al.* 2022; Allsop *et al.* 2023). The salt caverns at Clemens Dome and Moss Bluff are built in salt domes at a depth of 800 m, with volumes of approximately 580,000 m^3. Clemens Dome and Moss Bluff have operated since 1983 and 2007, respectively. These projects have operated under a long duration storage operational model and rarely cycle the gas frequently through the cavern, i.e. steady cavern pressure is maintained over long periods of time. This have unequivocally demonstrated for decades that underground hydrogen storage is a technically feasible option for long duration storage. Questions do remain, however, regarding the frequency of cycling and impact of quickly removing and replenishing gas over short periods of time in a salt cavern.

Further projects are planning to store hydrogen in salt caverns in the United Kingdom, including the HyKeuper project in Cheshire, storing 1.2 TWh by later this decade, and Aldbrough at Humberside storing of 0.3 TWh by 2028. Gas storage and brine caverns at Teesside are also being considered for the conversion to GWh-scales of hydrogen storage and evidence suggests they are oversubscribed to deliver the local capacity required (IDRIC, 2024). In Europe, the HyPSTER, Gasunie, RWE Epe-H2 and Salt-Hy projects also intend to further salt cavern hydrogen storage technology readiness.

When considering halite as a host for energy storage facilities, it is vital that the geological history of the target formation is characterised. A detailed understanding of the different depositional environments that created a salt deposit will provide information on a number of different physical aspects of the salt deposits including: lateral extent, depth and thickness, chemical variability, heterogeneity frequency, and potential impact of layers of different lithological composition interbedded in the salt deposits (e.g. carbonates). This will minimise the uncertainty in exploration and strengthen the prosperity of a target region.

The UK possesses important bedded halite deposits which are commonly associated with mudstone, anhydrite and/or other evaporitic minerals. The most extensive deposits, underlying the NE of England, are of Permian age and are constituent formations in the Zechstein (Fyfe and Underhill 2023a). Thick halite beds of Triassic age occur in NW England and the Cheshire, Stafford, Worcester, Somerset and Wessex Basins (Evans and Holloway 2009). Further salt deposits of Permian and, most importantly, Triassic age, are found in Northern Ireland, as proved in the Larne boreholes (Manning and Wilson 1975; Penn *et al.* 1983; Fyfe *et al.* 2020). It is understood that it is only the deposits in Wessex, Cheshire, Lancashire and NE England, and some offshore areas including Larne are of suitable depth, thickness and composition to host viable storage caverns. There are no known suitable salt deposits onshore in Scotland or Wales.

Numerous studies have estimated the required storage capacity and total theoretical capacity for hydrogen (Van Gessel et al., 2022; Kondziella et al., 2023; Chen et al., 2023; Tarkowski et

al., 2023 and references therein). Specifically for the UK, numerous authors have modelled the hypothetical energy storage capacity for salt caverns onshore and offshore UK. Evans and Holloway (2009) reviewed the potential locations for salt cavern placement in Permian and Triassic strata for both onshore and offshore considering methane storage. Caglayan et al. (2020) then produced Europe-wide model for Permian surfaces using standard volume for all of the Zechstein strata to calculate potential hydrogen storage, providing a first-order assessment of 9.0 PWh primarily located in the Southern North Sea. Williams et al. (2022), Allsop et al. (2023), Barnett et al. (2024) and IDRIC (2024) further refined the Caglayan et al. (2020) model using similar geological models for location and strata specific capacity estimates, providing 2.1 PWh, 61.9 PWh, 292 TWh, 22-48 TWh for various onshore and offshore basins around the UK. Each basin hypothetically has the capacity to provide ample storage far in excess of predicted requirements, however, all authors note that substantial refinement of each estimate is required to move beyond contingent resource estimates and turn a theoretical assessment into a realisable potential, depending on technical, social and economic viability.

4 Permian deposits in NE England and Southern North Sea, the Zechstein Supergroup

The full Zechstein evaporite succession comprises five depositional cycles, with a full cycle ideally including a basal mudstone that is overlain by a carbonate unit and evaporite (anhydrite/halite; Fig. 1). Some cycles are only represented by parts of this idealised cycle. The cycles are numbered from the oldest (Z1) to youngest (Z5), and incomplete or missing cycles are common due to structural complexity and non-deposition in parts of the Southern Permian Basin. This complexity results in difficulties in correlation where seismic or borehole well data is poor or missing. Figure 1 exhibits the stratigraphic sequence for the Zechstein comparing onshore and offshore nomenclature.

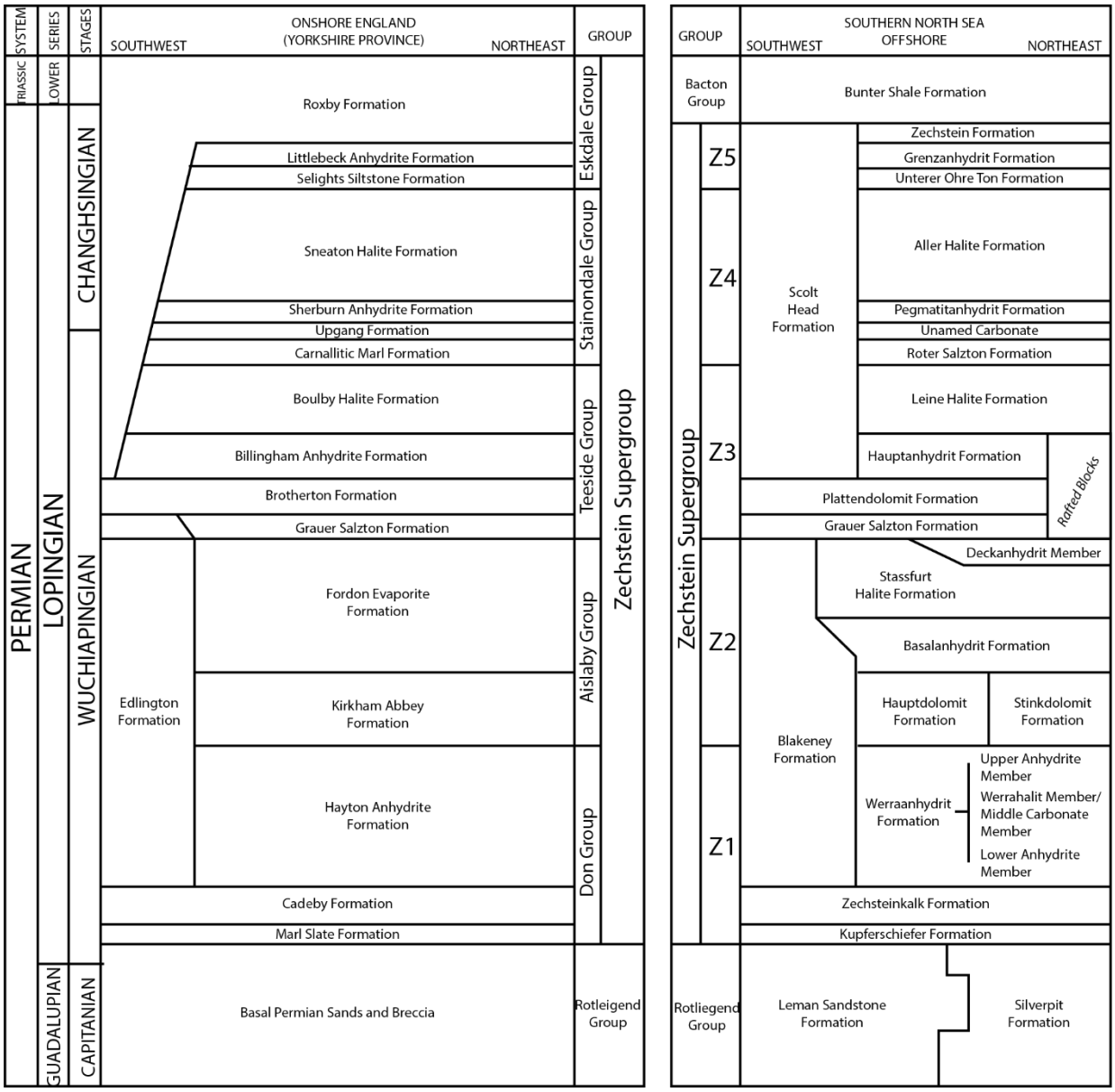

Figure 1. Stratigraphic column highlighting the different nomenclatures used for Zechstein formations offshore in the Southern North Sea and onshore NE England (Yorkshire), together with common abbreviations. Adapted after Fyfe and Underhill (2023a).

4.1 ZECHSTEIN 1: MARL SLATE, CADBEY AND HAYTON ANHYDRITE FORMATIONS

The Z1 is composed of the Marl Slate Formation, Cadeby Formation and Hayton Anhydrite Formation (offshore: Keuperschiefer, Zechsteinkalk, Werranhydrit). Initial Zechstein transgression in the Southern Permian Basin resulted in the deposition of thin, organic-rich shales with local high-carbonates, marls (Turner and Magaritz 1986; Smith 1989; Kotarba *et al.* 2006), resulting in the Marl Slate Formation. Overlying this is the Cadeby formation consisting of carbonites and locally mudstones that thicken basinward, with increasing depth of depositional facies (Fyfe and Underhill 2023b). A sudden change of salinity, perhaps relating to change of sediment influx, led to an abrupt basinwide change to sulphate deposition leading to the Hayton Anhydrite Formation (Cameron *et al.*, 1992; Smith 1989) on a shelf slope forming as a wedge. Locally, halite may be recorded in lozenge-shaped lensoid pods interpreted to have been deposited in shallow, saline pools (Underhill and Hunter 2008), however, these are no more than 50 m thick and only observed on shelf and not in basinal or slope conditions. Due to the lack of halite thickness and heterogeneous deposition of halite interspersed with anhydrite, the Z1 is thought to be unsuitable for cavern development.

4.2 ZECHSTEIN 2 KIRKHAM ABBEY AND FORDON EVAPORITE FORMATIONS

The transition to Z2 cycle is marked by an influx of marine waters into the Southern Permian Basin from the north, ending the deposition of Zechstein 1 sulphate-dominated sediments and re-establishing carbonate depositional conditions (Smith 1989; Johnson et al. 1994). There is significant variation in thickness and stratigraphy across NE England for the Z2 cycle (Fyfe and Underhill 2023b). The Kirkham Abbey Formation (Hauptdolomit offshore) is spread over most of the Southern Permian Basin with platform strata, from carbonates to ooidal and peloidal grainstones, mudstones, wackestones and organic-rich carbonates, dependent on platform, slope or basinal location.

Overlying this is the Fordon Evaporite Formation, marking a change from carbonate to sulphate deposition relating to evaporation of the transgressive marine influx. Initial anhydrite refines to halite with subordinate polyhalite, anhydrite, carnallite and kieserite (Johnson *et al.*, 1994). The thickest deposits of halite can be found basinward of the Z2 carbonate-evaporite shelf, bounded by a steep gradient shelf of carbonates bounding the basin on the southern and eastern margins. The location of the Z2 carbonate-evaporite shelf significantly influences the thickness of the Z2 halite. Basinward of the shelf, halite is typically between 200 m and 400 m thick although it can reach over 1 km in thickness offshore in the Southern North Sea as a result of salt tectonics and halokinesis. Halite deposited on top of the Z2 carbonate evaporite shelf is in general up to about 75 m thick.

Z2 halite thicknesses of over 200 m occur onshore near the coastline NE of Hull and SE of Middlesbrough. It pinches-out and transitions into the clastic-dominated, marginal-marine to continental Edlington Formation at a maximum distance of about 50 km inland from the coast, and the depositional limit of the halite is located between the cities of Hull and York. East of the English coastline the halite thickens offshore in the Southern North Sea and the effects of halokinesis can be observed on seismic profiles, resulting in significant salt structures such as domes, pillows and walls which cut through the overlying stratigraphy and areas of salt withdrawal (Allsop *et al.* 2023; Fyfe and Underhill 2023b).

There is a change in stratigraphy across NE England and the adjacent Southern North Sea. In offshore locations in more basinal palaeo-depositional settings, the typical Z2 stratigraphy consists of an anhydrite succession, in general less than 50 m in thickness (known as the Basalanhydrit Formation offshore), overlain by halite and polyhalite which is typically hundreds of metres thick (known as the Stassfurt Halite Formation offshore). Much of the original depositional textures being preserved within the polyhalite, indicating that the formation of polyhalite is likely caused by replacement of anhydrite and reaction with halite-precipitating brines containing potassium and magnesium (Kemp et al. 2016). In onshore locations to the west, where palaeo-depositional settings were more proximal, anhydrite becomes more common and the halite succession contain an increasing number of shale and anhydrite interbeds. These interbeds are typically localised and cannot in general be correlated between

wells/boreholes. West, between the cities of Hull and York, the Z2 halite is replaced by mudstones with thin anhydrite interbeds.

4.3 ZECHSTEIN 3 BROTHERTON, BILLINGHAM ANYHYDRITE AND BOULBY HALITE FORMATIONS

Similar to the Z2 cycle, there is a significant lateral difference in thickness and stratigraphy within the Z3 cycle. Another transgression and influx of normal-marine waters entered the Southern Permian Basin marking the start of the Z3 cycle (Johnson et al., 1994). The cycle initiates with the Brotherton Formation (offshore: Grauer Salston), a carbonate variable in facies and deposition dependent on shelf, slope or basin location.

As with previous Zechstein cycles, carbonate -dominated deposition was replaced by anhydrite deposition as salinity in the Southern Permian Basin increased through the Z3 cycle. Thus, the anhydrite-dominated (Billingham Formation; offshore: Hauptanhydrit)) was deposited and is 25-70 m thick in the basin centre and 15 m thick across the Z3 carbonate shelf (Cameron *et al.*, 1992). The Billingham Formation gave way to the Boulby Halite Formation (offshore: Leine), which was deposited across most of the Southern Permian Basin in response to increasing salinity. The formation is dominated by halite with subordinate polyhalite, carnallite, sylvite, anhydrite and mudstones, and thickens basin-ward to a maximum of 300 m (Cameron *et al.*, 1992). The Z3 cycle generally contains fewer interbeds and is thinner than the Z2 cycle, and the Z3 and Z2 evaporites are thickest in different onshore locations: Z3 evaporites are thickest SE of Teesside, whereas Z2 evaporites are thickest in the area between Withernsea and the Flamborough Head Fault Zone. Halokinesis has led to marked lateral variations in the formation's thickness (Johnson *et al.*, 1994).

4.4 ZECHSTEIN 4 AND ZECHSTEIN 5 CYCLES

Carbonate deposition decreased in the Southern Permian Basin and the area was dominated by evaporites formed in hypersaline conditions. The Roter Salzton Formation in the Z4 cycle are an Unnamed Carbonate Formation, the Pegmatitanhydrit Formation and the Aller Halite Formation, and the Z5 Unterer Ohre Ton Formation, Grenzanhydrit Formation and Zechsteinletten Formation (Grant *et al.* 2019). Z4 and Z5 cycle deposits are relatively thin or absent onshore and are difficult to distinguish from each other.

4.5 STRUCTURE OF THE ZECHSTEIN SUPERGROUP

Across the majority of eastern England and Southern North Sea, the Zechstein Supergroup has a general shallow easterly dip (Peryt *et al.*, 2010; Brackenridge *et al.* 2020; Fyfe and Underhill 2023b). Onshore, there is little structural deformation of the Supergroup with the exception of the Flamborough Head Disturbance, a complex fault system which separates the Cleveland Basin from the Market Weighton High, downthrowing the north. Significant halokinesis has been recorded offshore in deeper sections of the basin, resulting from overburden causing visco-plastic deformation. This has led to diapirs and walls rising to the surface in some places and is forms the structural trap for some Southern North Sea hydrocarbon fields.

5 Exploited Zechstein deposits onshore UK

5.1 BOULBY MINE

Boulby is located on the east coast of North York Moors, close to the boundary of Cleveland and North Yorkshire. Since 1973, potash has been extracted from the mine from the Z3 more than 1100 m below sea level (Woods 1979; Talbot *et al.* 1982), and is currently operated by ICL Group Limited. The primary target of the mine is the Boulby Potash (Fig. 2), containing similar proportions of sylvite (KCl) and halite (NaCl) with some insoluble material including clays and anhydrite. The mining operations extend 12.5 km, reaching 5 km offshore to the north where they are approximately 800 m below the seabed (Wrighton and Bide, 2013).

The potash is bounded by the Boulby Halite underneath and succeeded by the Carnallitic Marl. The Boulby Potash has been subject to mobilisation from chemical dissolution and precipitation, and mechanical movements by thrust faulting, folding and halokinesis. The Boulby Potash averages 7 m in thickness but ranges from 0 to over 20 m. The member consists of sylvinite (a mixture of sylvite and halite) with minor clay minerals and anhydrite, and traces of other minerals. The material mined is of high-grade by international standards with a mean KCl content of 34%. However, grade varies both vertically and laterally (Wrighton and Bide, 2011). A substantial resource of polyhalite is also found within the Boulby Potash, however the extent, grade or thickness of this mineral horizon has not been published.

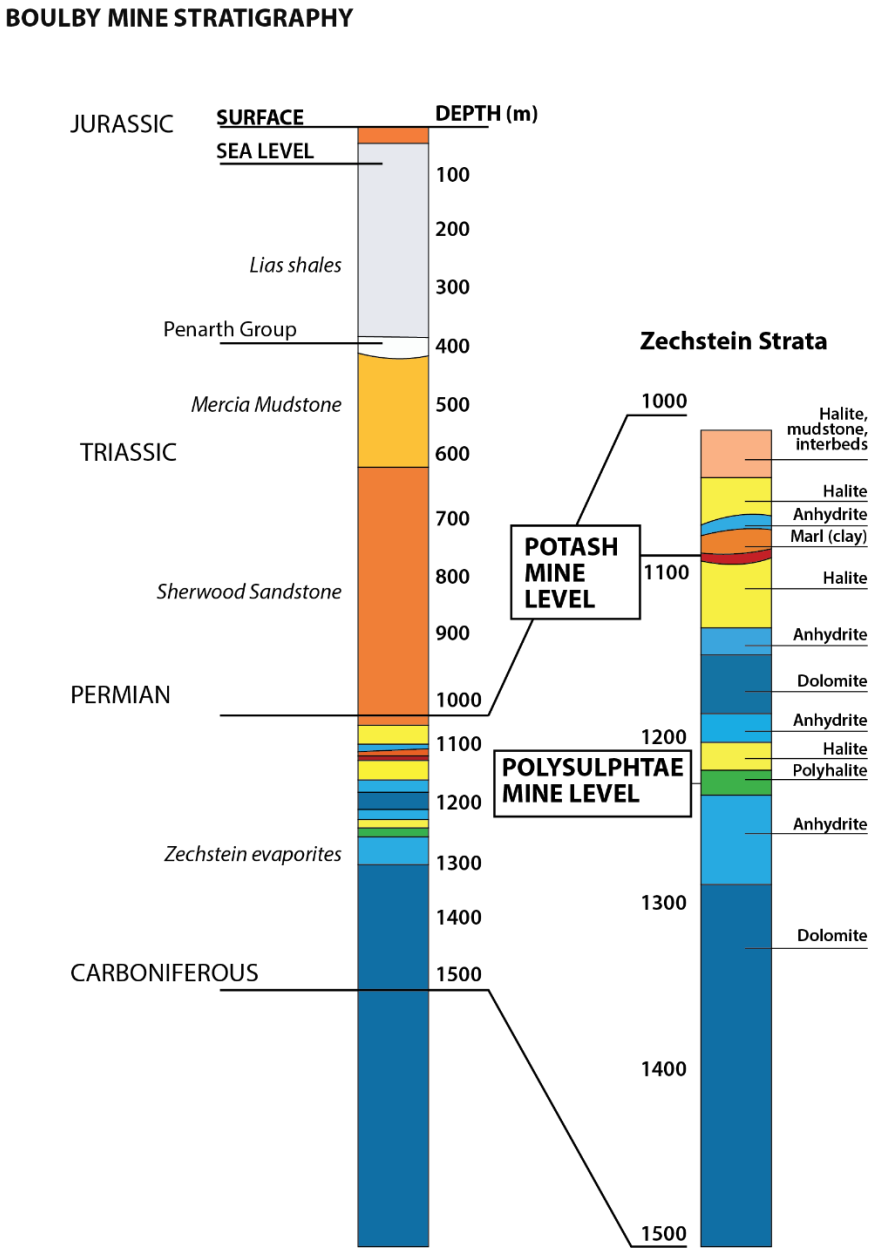

Figure 2. Stratigraphic column for the Boulby Mine, located within the Zechstein Z2. Adapted after ICL (2018).

At Boulby, the Boulby Halite is 50 -+15 m thick, consisting of massive halite with some subordinate mineral assemblages. Structurally the Boulby Halite is undisturbed expect for isolated faults extending from the underlying anhydrite and dolomite formations. The uppermost 3-4 m of the halite is generally brownish grey with locally speckled sylvite. Moving downwards, halite crystals are generally larger. Within the halite, a sharp contact separates a greyish halite from an orange-pink halite with low sylvanite content, which provides a distinct marker throughout the mine. Below this is a coarse orange-brown halite wit interstitial grey clay showing desiccation cracks and infilled solution cavities. The cracks are dark grey argillaceous halite. Further below this, the Boulby Halite shows increasing anhydrite content, first as minor layers then increasing intercrystalline content until a contact with the underlying Billingham Anhydrite (Woods 1979).

Beneath the Boulby Halite are magnesium limestones, perhaps 200-300 m thick with minor Hayton Anhydrite and Kirkham Abbey Formation (Woods 1979; Smith 1996). The Boulby Halite is found as a unit of pure massive halite, which is used as the mine's main arterial roadway. The rock salt used in the production of these roadways is suitable for road salt.

Based on the marked variation in thickness of the Boulby Halite across onshore NE England and the assumption that the Boulby Halite was uniformly deposited, it is thought that salt mobilisation has occurred likely on the order of a few hundred metres laterally and dozens of metres vertically, causing thickening and thinning of the Boulby Halite and in places repetition of units (Smith 1996).

In the area south of the mine normal faults related to a phase of post-Triassic extension are interpreted on seismic lines to offset the top salt by c. 300 m, while at base salt very little offset is observed (Davison 2009). Thrust faults are also observed, likely related to the same inversion event, which have caused repetitions of horizons in the mine. In places, evaporitic units have a gneissose fabric with grains with 3:1 axis ratio, developed in response to structural deformation. In the north of the mine a dark argillaceous halite forms a horizon 5–6 m below the top of the halite.

Talbot *et al.* 1982 also describes veins, vein networks, shear zones and asymmetric sub-horizontal lobes of gneissose sylvinite that root in and repeat the first formed layer in structures that developed to various degrees in different parts of the mine. They envisaged a measure of semi-liquefaction to account for the severe folding of parts of the Boulby Potash and uppermost Boulby Halite in Boulby Mine. The process, perhaps driven by volume and temperature changes during the transition from gypsum to anhydrite along with the water released in these transitions, caused dissolution and softening of some halite and sylvite, which was flushed out into fractures in the base of the overlying impermeable Carnallitic Marl. This brine movement could have been triggered by rifting in Triassic times (Talbot *et al.* 1982).

Concurrent to being a working potash mine, Boulby hosts the Boulby Underground Laboratory (BUL) approximately 1070-1100 m below ground surface, which was initiated in 1988. BUL was created to investigate dark matter, which requires low background radiation conditions. Since then, BUL has expanded to include a number of other experiments and testing facilities that require minimal cosmic radiation. The BUL instillation shows the collaborative community within the ICL mine site, being a place for multidisciplinary scientific investigations.

The ambient conditions underground are hot and dry; the air temperature is 28°C but rises to 35°C where it is unaffected by mine circulation (Daniels et al., 2023). The mine roadways are situated in the Boulby Halite and the proximal stratigraphy includes other Permian evaporites. The lithostatic pressure at BUL is 28 MPa and there is no obvious deviatoric stress within the rock mass, other than the decompressed region around the gallery openings (Daniels *et al.* 2023).

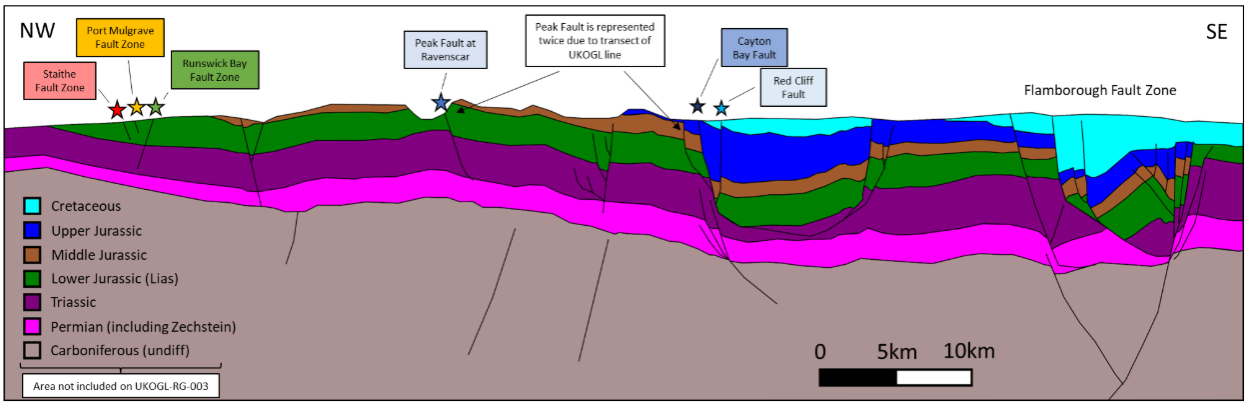

Figure 3. Schematic cross section of the Cleveland Basin, NW-SE, including York Moors and Humber and Wash regions. Adapted after Lee (2023), a reinterpretation of a UKOGL regional seismic line.

5.2 WOODSMITH MINE

Woodsmith Mine is being developed on the East coast of the North York Moors, close to Whitby and within the National Park boundaries. The mine targets polyhalite, predicting a total reserve of 2.66 bn t of resource, with 280 m t of reserves within a 5 km radius of the mine site location. The mine is located within the second Zechstein cycle (Z2 Fordon Evaporite Formation), approximately 1600 m below ground level. The only known occurrence of polyhalite in the UK is within this sequence, and although the polyhalite is not an uncommon mineral, it is extremely unusual to find it in such mineable quantity and quality (Kemp *et al.* 2016).

Polyhalite was described in the Eskdale and Fordon boreholes as partly primary but mainly as a replacement mineral for primary anhydrite in Fordon Z2. The lower sub-cycle was deposited in a basin that still displayed considerable topographic variation from a shallow-water shelf to a deepwater basin. It contains no known potash occurrences. The middle sub cycle, in which the polyhalite occurs includes a large volume of basin-fill evaporites, chiefly halite, which filled and smoothed out the shelf-basin geometry. Consequently, it shows considerable variation in thickness. The upper sub cycle formed in uniformly shallow-water conditions with no clear distinction between shelf and basin. Mining is thus focussed on the middle horizon, with an average thickness >12 m for high grade (>85% polyhalite) sections (Kemp *et al.* 2016).

To avoid disruption to the National Park, a 37 km long tunnel is being constructed that would convey the polyhalite from the site to Wilton, Teesside, for processing and export. Once completed, this will be the longest underground tunnel wholly within the UK. Tunnelling will face a mixture of geological conditions but will minimise geotechnical variations by remaining relatively parallel to bedding. Several fault zones have been identified that will cross the tunnel (Gschnitzer *et al.* 2020). The tunnel is primarily located within the Redcar Mudstone Formation, an impermeable horizon that avoids disruption to local aquifers.

5.3 SALT CAVERNS

The salt caverns at Atwick and Aldbrough in north Humberside are located in the Z2 Fordon Evaporite Formation. The caverns were developed in halite over 200 m thick at depths between 1730 and 1900 m. Further west towards York, the formation thins before pinching out entirely. Salt caverns developed to the east would have to be located offshore, leading to higher costs (the potential for developing salt caverns offshore has been investigated by Allsop *et al.,* 2023). To the north of the Atwick and Aldbrough caverns is the east-west oriented Flamborough Head Disturbance (or Fault Zone) (Roberts *et al.* 2020). Structural deformation associated with the fault zone decreases significantly to the south, reducing the potential of faults which could affect cavern integrity.

One area with significant potential to host storage caverns within the Z2 Fordon Evaporites is located close to the pre-existing caverns at Atwick and Aldbrough, in the coastal region north of Withernsea but south of (and unaffected by) the Flamborough Head Fault Zone. In this region, Z2 halite is over 200 m thick and occurs at depths between 1000 m and 2000 m.

In the Teesside area in NE England, the Z3 evaporites were initially exploited for brine extraction in the late 1800s and early 1900s at Saltholme and Wilton (Evans and Holloway 2009; Williams *et al.* 2022). Brine extraction resulted in cavern formation, with some caverns later converted into sites for the storage of light hydrocarbons, propane, propylene, crude oil, gas oil, naphtha, ethylene, nitrogen and hydrogen (Beutel and Black, 2005; Evans and Holloway 2009). The salt caverns at Wilton are 650 m below the surface and those at Saltholme 340 m below the surface (Evans and Holloway 2009). The caverns are located on the very northern margin of Z3 evaporite deposition. The Z3 evaporites in the Teesside region are relatively shallow (typically less than 500 m deep) and are relatively thin; thicknesses are up to 40 m, increasing to around 60 m to the southeast and to over 100 m in offshore areas around 40 km east of the coastline.

6 Existing data for Boulby Mine

To increase our knowledge of the geology at Boulby Mine, it is necessary to understand what primary geological data is held by the BGS or is accessible in the public domain. This is completed by a data discovery exercise, which has identified key boreholes, seismic and geomechanical reports on the Boulby Halite. Below is a summary of the geoscientific data collected on Boulby Mine.

6.1 BOREHOLES

A search for boreholes that have been drilled onshore and offshore near (<5 km) Boulby that intersected the Z3 Permian halite was conducted using the UK Onshore Geophysical Library (UKOGL) webmap and North Sea Transition Authority (NSTA) National Data Repository. A similar search was also conducted with core held at the BGS core store. In total, this has revealed 6 boreholes that may be of use, as listed in tables 1-3. Four boreholes are held with UKOGL and one with BGS. Two of these boreholes have accessible logs, Staithes 1 (NZ71NE/9) and Boulby Watchman (NZ71NE/64). Offshore, no boreholes directly intersect the Permian near the mine. The closest well drilled is 41/08-2.

UKOGL ID	Well Name	OGA Reference	BGS Reference	Operator	Spudded	Completed
669	STAITHES 1	L41/11- 2	NZ71NE9	HOME	20 Sept 1965	06 Oct 1965
4510	STAITHES 2 BH	-	NZ71NE18	ICI	1966	1966
4834	BOULBY MINE SHAFT 1	-	NZ71NE23	CLEVELAND POTASH	1969	1970
4511	STAITHES 3 BH	-	NZ71NE17	ICI	1966	1966
-	Boulby Watchman (underground borehole)	-	NZ71NE/64	ICL	-	-
-	41/08-2	-	-	HABOUR ENERGY PLC	24 Dec 1994	28 Jan 1995

Table 1. Summary of publicly accessible wells drilled proximal to the BUL facility or within Boulby Mine.

6.1.1 Staithes 1

Staithes 1 borehole was drilled by Home for Imperial Chemical Industries for potash in the Permian Upper (Z4: Carnalitic Marl, Upgang Fm, Sherburn Anhydrite, Sneaton Halite) and Middle Evaporite (Brotherton Limestone, Billingham Anhydrite, Boulby Halite) beds. Home Oil then deepened the well to the top Carboniferous as a wildcat test for hydrocarbons. The borehole is located onshore between the Boulby surface facility and Staithes. The borehole was vertically drilled to a total depth of 1516 m bgl, and contains induction electrical, microcaliper, gamma ray, sonic, cement bond, temperature and mud logs. No lithological log exists above the Bunter Shale-Sandstone contact at 2852', with these tops inferred from the gamma log. The well intersects the surface Jurassic, Penarth and Bunter Triassic, Zechstein Permian and Upper Carboniferous, as summarised in Table 2. A more detailed log for the Zechstein Supergroup is given in Table A1-3. In summary, the top Zechstein Littlebeck Anhydrite is intersected at 955 m, with the bottom Zechstein at 1434 m, marking a total thickness of 479 m. The Boulby Halite is merged with the Billingham Anhydrite, and the upper contact with the Carnalitic Marl is listed as unknown due to a gap in the log. Staithes 1 intersects the top and bottom of these groups at 1013 m and 1100 m respectively, totalling 87 m thickness.

Formation Tops	MD (ft)	MD (m)	Thickness (m)
Littlebeck - Sneaton	3134	955	58
Carnalitic Marl – Boulby Halite – Billingham Anhydrite	3325	1013	87
Brotherton	3608	1010	30
Fordon Evaporites	3706	1130	99
KAF	4030	1228	94
Hayton	4340	1323	91
Cadeby	4640	1414	40

Table 2. Formation tops for Staithes 1 borehole.

6.1.2 Boulby Watchman

The Boulby Watchman Borehole was drilled to further understand the lithology, thickness and structure of the Boulby Halite to expand and develop Boulby mine. The Table 3 presents a summary for the borehole before a detailed description of the core held by the BGS is given. Of note, the borehole was drilled vertically downwards from -1100 m below ground level, to a length of 46.5 m. The borehole intersects the Boulby Halite and Billingham Anhydrite, showing variation in the petrology for halite through section.

UKOGL Well ID	-	Operator	ICL
Spud Date	-	Completed Date	-
Surface Location (BNG)	X=477841 Y=518270	Deviated	No
Measured Depth Datum	Kelly Bushing	Original Depth Units	Metres
Datum Elevation	-1100m bgl	Depth of borehole	46.5
Surface Formation	Boulby Halite	Surface Formation Age	Permian

Table 3. Formation tops for Boulby Watchman borehole.

The 46.5 m-long Boulby Watchman core was scanned at the Core Scanning Facility (CSF) at the British Geological Survey (BGS). The comprehensive core scan dataset (BGS Core Scanning Facility, 2024) consists of high-resolution optical and radiographic images, geophysical multi-sensor core logger and geochemical X-ray fluorescence (XRF) point data of the whole round bare rock core, as well as computed tomography (CT) scans of three selected core sections (Table 4).

Table 4. Boulby Watchman Core Scanning Datasets

Scan	Core scanned
Optical Imaging	0 – 46.5 m
Radiographic Imaging	0 – 46.5 m
Computed Tomography (CT)	12.5 – 13.5 m 31.5 – 32.5 m 38.5 – 39.5 m
Multi-Sensor Core Logging	1 – 46.5 m
X-Ray Fluorescence (XRF)	20.5 – 46.5 m

High-resolution optical images were collected using a Geotek Geoscan V colour line-scan camera mounted on a Geotek core workstation. Pixel resolution is 50 microns. The images will provide the user with information on the visual characteristics of the core (e.g., colour, structure, alterations) and can be used for detailed core quality assessments (Figure 4).

Figure 4. High-resolution optical imaging of the Boulby Watchman core obtained at the Core Scanning Facility (CSF) at the BGS. Core images at 4.5 m, 32.5 m, 36.5 m, and 43.5 m drillers depth, respectively.

2D X-ray images were collected using a Geotek rotating computed tomography (RXCT) core scanner. Pixel resolution is 42 microns. Radiographs were collected at two angles (0°, 90°) to give the user information on how features propagate through the core. Radiographic images will provide the user with information on the internal and structural characteristics of the core (e.g., fractures, bedding structures, deformation features) (Figure 5). Radiodensities can be used to differentiate between halite and anhydrite lithologies.

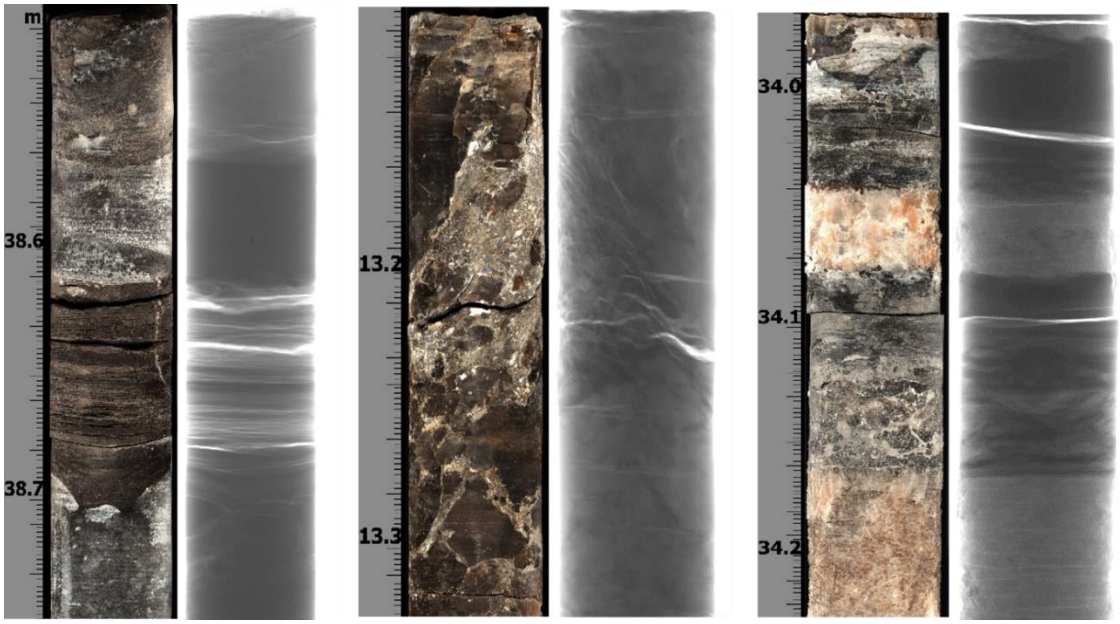

Figure 5. Optical and radiographic images of the Boulby Watchman core obtained at the Core Scanning Facility (CSF) at the BGS.

CT images of three selected core sections were collected using a Geotek RXCT core scanner. The CT dataset combines a number of 2D scans taken at 0.1° angle increments to produce cross-sectional images and two orthogonal downcore views at 0° and 90°. The slice views are used to produce full 3D reconstructions of the core sample so that three-dimensional structures can be visualised (Figure 6). CT can be used to visualise and quantify core features (e.g., pore space, anhydrite impurities, fracture networks, deformation textures).

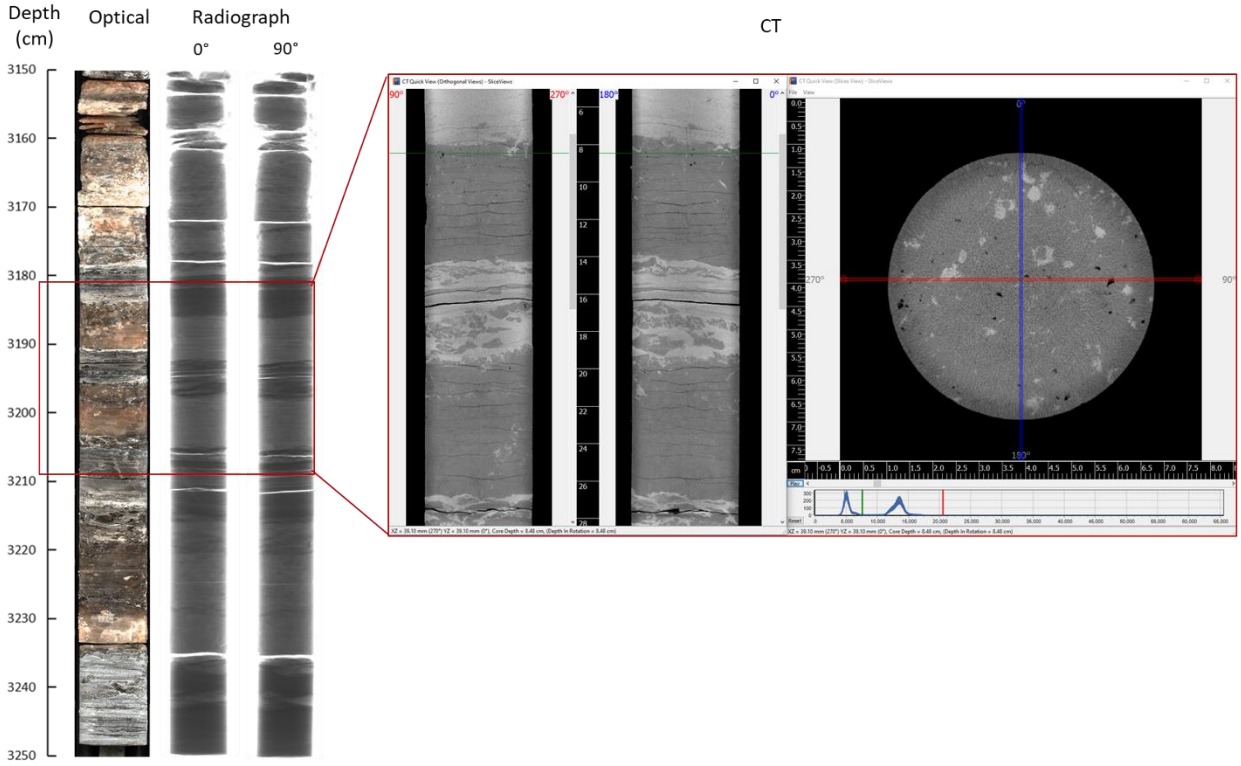

Figure 6. CT example of the Boulby Watchman core obtained at the Core Scanning Facility (CSF) at the BGS.

Geophysical point measurements, including gamma attenuation density (AG), P-wave velocity (PW), magnetic susceptibility (MS), and natural gamma activity (NG) were collected using a Geotek multi-sensor core logger (MSCL-S). The different physical property sensors were set to different step and exposure conditions, with AG, PW and MS set to a 1 cm step-size and 5 s exposure and NG set to a 5 cm step-size and 60 s exposure. XRF point measurements were collected at 2 cm intervals and 5 s exposure using a Geotek XYZ Core Workstation. The XRF data was acquired with no filter at 10kV for low Z range elements (Na-Co) and with a 25-micron silver filter at 40kV for high Z range elements (Ni-U). XRF elemental data is reported as raw counts (peak area). The raw count data provides an indication of variation in elemental abundances along the core but is not a quantitative analysis (Figure 7).

Geophysical and geochemical data is fundamental to the understanding of rock properties and their behaviour. Core scan data can help to resolve new relationships between physical and chemical properties and can form the framework for field and laboratory geotechnical test data.

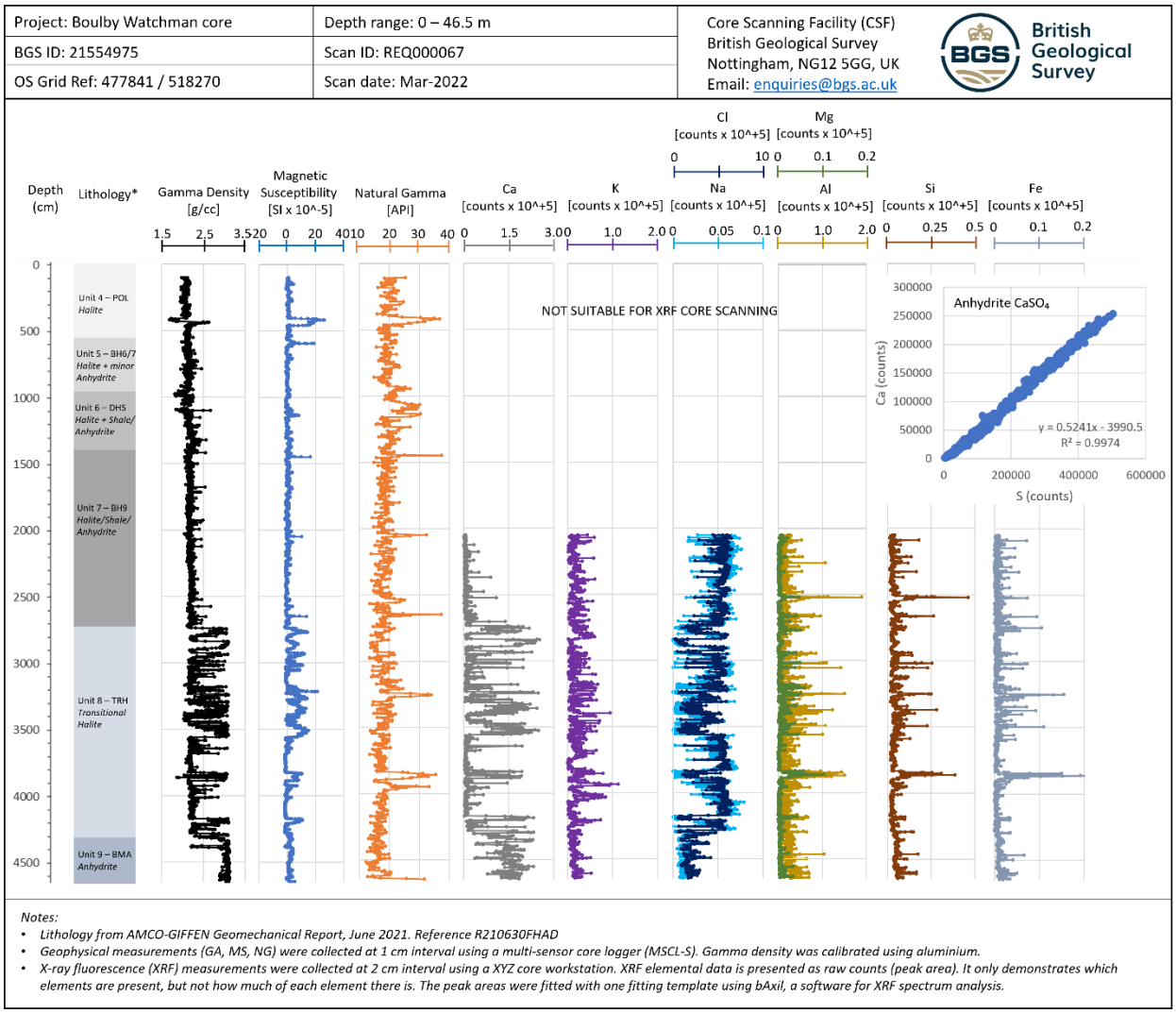

Figure 7. Geophysical and geochemical point data of the Boulby Watchman core obtained at the Core Scanning Facility (CSF) at the BGS.

6.2 SEISMIC

Seismic was shot in the Boulby vicinity between 1981-86 by Shell during oil and gas exploration of the area. Of interest, seismic line (SY82-10V) was shot in 1982 directly above the Boulby facility. Various lines also run perpendicular or parallel to line SY82-10V that may give indication as to the wider basin structure. A summary for line SY82-10V is provided in the below Table 5.

Line name	SY82-10V
UKOGL ID	17442
Operator	SHELL
Vintage	1982
SP/CDP range	101 to 1862
Length (km)	22.45
Shot by	SSL
Source	Vibroseis
Survey ID	SH822DL004

Table 5. Summary information for Shell seismic line shot near Boulby, SY82-10V.

6.3 GEOMECHANICAL MEASUREMENTS

As part of a series of appraisals for the development and expansion of Boulby Mine, including ground investigation and drilling works, three geomechanical characterisation reports have been sourced on the physical properties of the rock salt located at Boulby Mine (Clausthal 2021; Hadj-Hassen 2021; Solexperts GmbH 2021). The following section summarises the findings for these reports.

6.3.1 Geomechanical characterisation

Hadj-Hassen (2021) characterised the geomechanical features of the Boulby Halite and Billingham Anhydrite, including measurement of the physical properties (density and sonic velocity) using Brazilian tests, uniaxial and compression triaxial tests and multistage triaxial creep tests on the rock salts.

6 rock types were identified based on the core provided, five halite and one anhydrite unit, with sub samples collected from each. Lithological descriptions and depths are listed in Table 6. A summary of the results is made in Table A4-A5 and in the following statement.

Overall, the results indicate the average tensile strength is *c.* 1.5 MPa, while unconfined compressive strength is more variable, from 19-25 MPa dependent on the halite heterogeneity, and 42.9 MPa for the anhydrite. Similarly, Young's modulus is variable with anomalous 28.2GPa and lower values of 21.7 GPa and 10.5 GPa. For anhydrite, the average Young's modulus deduced from uniaxial and triaxial compression tests is 55.4 GPa. Poisson's ratio is variable for the different rock salts and depends on the rate of insoluble materials, from 0.21-0.29 for halite to 0.31 for anhydrite. Average deviatoric stress is 35 MPa for halite, while a shear criterion was used to describe the compressional failure of the anhydrite with an unconfined compression strength of 59.1 MPa, confinement coefficient of 3.7, cohesion of 15.4 and friction angle of 35^{o}. Based on the results of the creep tests and the associated calculated creep indexes, it is possible to consider that the rock salts of the Boulby site are relatively low creeping halite rocks.

Depth (m)		Lithology	Description
From	To		
0.00	5.36	Polygonal Halite	Medium strong - strong orange, brown occasionally colourless translucent coarse-grained Halite. Crystals generally 5-10 mm, rarely up to 30 mm in size. Occasional to frequent orange-red iron staining. Rare distributed soft grey siltstone in 1-20 mm pockets, occasionally appearing as 1-5 mm irregular bands crosscutting the core. Within upper 3-4 m of core logged, iron staining is frequent, and rare white anhydrite randomly distributed throughout. The lower 3-4 m of logged core sees anhydrite becoming occasional to frequent. Fractures all drilling induced stress release fractures
5.36	9.86	BH6/BH7	Strong dark grey, grey, brown and orange occasionally translucent/colourless coarse grained silty anhydritic Halite. Anhydrite is fine grained. Frequent thin weak siltstone randomly distributed throughout core, and also found as pockets 1-10 mm. Occasional to frequent brown iron staining. Boundary between geological unit BH6 and BH7 is gradational; BH6 contains approx. 30% silt, 10% anhydrite and 60% halite. Anhydrite content is greater in BH7. Fractures are drilling induced stress release fractures,
9.86	13.90	Dirty halite and shale bands	Strong dark grey, grey, orange-brown and colourless interbedded fine to coarse grained silty anhydritic Halite and thin siltstone. Interbeds of dark grey fine siltstone, fine silty anhydrite and very coarse halite. Siltstone can occur as pockets up to 40 mm and as bands frequently occurring as 1-20 mm thickness throughout core, randomly oriented enclosing halite crystals in a "pegmatitic" texture. Distinct bands can be 10-15 mm thickness, horizontal in orientation. Siltstone bands have swollen since coring. Halite crystal overgrowths noted throughout with individual crystals up to 35 mm. Crystals show no preferential orientation. Anhydrite "stringers" occur occasionally as randomly orientated 1-5 mm thickness. Fractures are all drilling induced.
13.90	27.88	Dirty halite	Strong dark grey, light grey, orange-brown and colourless fine to coarse silty anhydritic Halite/silty halitic Anhydrite. Occasional to frequent distinct siltstone beds 1-10 mm thick spaced throughout section. No "pegmatitic" texture of siltstone+halite crystal overgrowths. Fractures are drilling induced,
27.88	43.04	Transition zone halite-anhydrite	Strong dark grey, light grey, colourless, orange brown thickly interbedded fine to coarse Anhydrite + Halite. Anhydrite bands are strong, dark grey and white, fine to medium. Weak foliation/fabric in some of the anhydrite layers (not all) very closely to closely spaced inclined 45°. Halite bands are strong orange-brown and rarely colourless coarse with occasional anhydrite+siltstone inclusions 1-20 mm in size dispersed randomly. No structure. Fractures are drilling induced.
43.04	46.50	Billingham Main Anhydrite	Strong dark grey, light grey and white fine to medium Anhydrite with some dolomite. Horizontal beds of anhydrite-dolomite noted between 43.5-43.8 m and 45.4-46.5 m.

Table 6. Summary table for lithological descriptions and geomechanical tests on the Boulby Halite and Billingham Anhydrite (after Hadj-Hassen, 2021), linked to lithological description provided in Section 5.1

6.3.2 Creep behaviour rock salt

Clausthal (2021) conducted 5 triaxial long-term tests to evaluate the creep properties of rock salt samples from Boulby Halite. Measurements for longitudinal (p) and shear (s) waves were taken to infer dynamic elasticity modulus, dynamic Poisson's ratio and density. Creep tests under triaxial compression were conducted in the long-term pressure balances up to 20 MPa and 40 ^{o}C. Calculations were also made for Norton's Parameter A and n. Table A6 presents a summary of these findings.

6.3.3 Hydraulic fracturing stress measurements

Solexperts GmbH (2021) carried out hydraulic fracturing stress measurements for the 45 m deep vertical borehole PQ05 drilled from -1100 level. A total of 10 hydraulic fracturing / hydraulic injection tests including 10 impression packer tests was conducted in borehole PQ05 between 6.5 m and 41.0 m MD (1106.5 m and 1141.0 m TVD). The derived characteristic pressure data (breakdown pressure Pc at fracture initiation, fracture re-opening pressure Pr, the resulting in-situ tensile strength T = Pc - Pr, and shut-in pressure Psi) are summarized in Table A7.

Only two of the 10 conducted tests are characterised by fracture initiation events with breakdown pressure values between 25.0 MPa and 30.8 MPa. The tests yield reliable fracture-pressure values between Pr = 15.4-16.6 MPa and Pr = 23.0-25.1 MPa. The hydraulic tensile strength varies between 6.5 MPa and 6.9 MPa. The distinct shut-in pressure varies between

16.6 MPa and 30.2 MPa. Both, refrac- and shut-in pressure show a significant increase between 6.5 m and 20.0 m depth, characterising the excavation-induced stress redistribution above this level. Between 20.0 m and 41.0 m, almost constant shut-in pressure values of 27.3 ± 1.7 MPa were observed.

7 Geomechanical and thermodynamic research in hydrogen storage in salt caverns

Operators of gas (methane, CAES or hydrogen) caverns are increasingly interested in using pressure cycles on the order of months, weeks or perhaps even days; these can be much shorter when compared to previous operating models of typically seasonal injection and production for methane storage. As a result, investigation as to the effects of the shorter stress and thermal cycles on the creep behaviour, dilatational potential and damage accumulation of salt are required to accurately model the impact of fast-cycle cavern operations. The following section is a summary of research conducted by the Solution Mining Research Institute (SMRI) on the topic of geomechanical and thermodynamic constraints in cyclic operation for salt caverns, specifically for hydrogen storage.

7.1 GEOMECHANICAL DATA FOR THE UPPER PERMIAN BEDDED HALITES

The Zechstein Z2 and Z3 cycles are bedded halites that have been used to construct gas and liquid petroleum storage caverns in East Yorkshire (Hornsea and Aldbrough: Z2) and on Teesside (Z3). A general lack of geomechanical data exists for Permian halite, however, and little is published in the public domain.

On Teesside, many storage caverns are repurposed former brine caverns and were not specifically designed for storage purposes. They were also constructed in the 1970's, and the geomechanical data acquired is not publicly available. However, a series of parametric studies were undertaken for Cavern 99, currently operated by SABIC UK Petrochemicals in the North Tees site, for a wet storage facility (liquid propane; Passaris and Noden, 2011). The geomechanical modelling was undertaken in order to investigate the potential for tensile failure in the roof of Cavern 99, constructed in the Boulby Halite and the roof of which is formed by the overlying Carnallitic Marl ('Rotten Marl') at a depth of 345 m below ground level. This is summarised in the Table 7 below:

Rock Type	Mechanical Property	Percentage of introduced change	Increased magnitude	Reduced magnitude
Boulby Halite (Z3)	*E* (MPa) Young's Modulus	40%	5139	2203
	T (MPa) Tensile Strength	40%	2.240	0.960
	v Poisson's ratio	25%	0.462	0.198

Table 7. Range of geomechanical properties for rock types used in the study of Cavern 99 on Teesside. (Passaris and Noden, 2011).

7.2 INDUCED STRESSES IN CYCLIC STORAGE CAVERNS

7.2.1 Cycling compressional stress and extensional-compressional states

Understanding the cyclic loading under compressional and tensional conditions are key to predicting salt cavern responses to cyclic storage of gasses. Mellegard and Dusterloh (2012) evaluated the effects of cyclic triaxial stress during triaxial compression creep tests on salt specimens from the Avery Island Mine in Louisiana. The Avery Island Halite is a domal Jurassic-aged relatively pure halite. Two states were tested during the experiment, 1) stress conditions remained below the dilation limit and (2) stress conditions cycled across the dilation limit. Ultimately, Mellegard and Dusterloh (2012) found that rapid cycling between dilatant and non-dilatant stress states caused microfracturing, but not enough to prevent recovery processes.

Mellegard (2013) then evaluated the impact of cycling axial stresses in triaxial extension and triaxial compression during creep tests. Similar core was collected from Avery Island Mine in Louisiana to allow for comparison between studies. The overall strain behaviour for the TXE cycle test was almost identical to the previous TXC cycle tests, except that the sign was the opposite (i.e., the specimen elongated rather than shortened).

The results of these experiments imply essentially zero strain, and that cycling between compressional and extensional is similar between compressional values under comparable test conditions.

7.2.2 Coefficient of thermal expansion

The coefficient of thermal expansion refers to the rate at which a material expands with increase in temperature under constant pressure and without phase change. Understanding the rate of expansion for halite is key for cavern operation to accurately model the thermodynamic response to loading and unloading. Buchholz et al. (2020) investigated the thermal expansion coefficient of damaged and undamaged salt under confinement using Avery Island Mine, Louisiana, halite. The research suggested that the thermal expansion coefficient did not change with damage, however, the results were mostly inconclusive.

This finding was confirmed by Buchholz et al. (2023), who found that thermal expansion coefficient shows quasi-constant values that do not change with varying degrees of damage. The value of the coefficient of thermal expansion is approximately 4.0×10^{-5} per ^{0}C for the Avery Mine halite.

7.3 TIGHTNESS OF ROCK SALT WITH REGARD TO HYDROGEN

Similar to gaseous hydrocarbon storage, hydrogen storage will require salt caverns to be gas tight to avoid any leakage. Berest et al. (2019; 2021) note that although leakage events are recorded in the salt cavern storage cases, almost all of these leaks are related to (1) a breach in steel casing at a depth where a single casing was isolating the stored product from the geological formations or (2) the presence of anomalous zones within the salt or overburden. A poor cementing job, weak casing connections, or excessive salt creep can lead to a breach of casing integrity. Pressure connection between caverns may theoretically occur if a non-salt layer (e.g. mudstone) or a highly soluble layer is intersecting the cavern and extending to the neighbouring caverns and/or to the edge of the salt structure, however, there is no record evidence of this happening.

Schlichtenmayer et al. (2015) measured salt permeability to nitrogen, hydrogen and methane at the finding that there is practically no difference in permeability of rock salt between these mediums. Ideally, in situ permeability tests may be conducted to confirm tightness, but based on the available literature no differences between the tightness of rock salt towards hydrogen and natural gas should exist. While a salt cavern can be considered as gas tight, the well and potential heterogeneous zones within the rock salt can be identified as the only potential weak points of the whole cavern system (e.g. Field et al. 2018).

7.4 CAVERN GEOMETRY AND OPERATIONAL PARAMETERS

Generally, the cavern design must be adapted based on the thickness, composition and material properties of the available salt section, and is dependent on local geology. There are several reviews of the concept for the design of caverns (e.g., Parkes et al., 2018; Evans et al., 2009; Caglayan et al., 2019; Williams et al., 2022; Alsop et al., 2023; Liu et al., 2023) and includes the determination of following design parameters:

- Cased roof pillar
- Uncased roof pillar
- Cavern volume
- Cavern diameter
- Cavern height
- Shape of cavern sump
- Shape of cavern roof
- Salt pillar between caverns

Similar to natural gas storage, cavern pressure in hydrogen storage has upper and lower limits, largely influenced by the lithospheric pressure exerted by overburden to a cavern. The maximum pressure is often referenced to the depth of the last cemented casing shoe and is dictated by the fracture gradient of the rock. Commonly, the maximum pressure is preliminary determined based on the formation pressure gradient minus a safety discount. This may typically be 80% of lithostatic pressure (e.g., Parkes et al., 2018). In order to guarantee the long-term stability of a cavern and to avoid damage, a minimum pressure limit is established, typically 24% lithostatic pressure (Alsop et al., 2023).

Creep rates must also be considered during determination of operational pressure range. As creep rate increases with pressure and temperature, it could be necessary to modify the operation of a cavern e.g., restrict cycling to only the upper pressure range, or to operate a cavern in “brine compensation mode” to avoid cavern volume reduction. There is no obvious reason for considering that the cavern pressure limits should be different for hydrogen, compared to common practice existing for natural gas.

Research gaps do arise on the consequences of fast cycling for caverns, as has been highlighted by Hydrogen TCP report (2022) Task 42. Little research has been completed as to the impacts of the pressure and induced temperature changes (Joule-Thomson effect) applied to the cavern and associated creep rate. Therefore, the geomechanical implications are unknown on rates of extraction and repressurising.

7.5 THERMODYNAMIC MODELLING

Thermodynamic modelling results for hydrogen operations are extensively presented in the literature, and the following section is a commentary of the following papers (Karimi-Jafari, 2016; Louvet et al., 2017; Minas and Skaug, 2021; Nieland, 2008).

When using volumetric or molar units, which represents the volume constraints of a cavern, the specific heat capacity of hydrogen is lower than for natural gas. That means that hydrogen needs less heat input to increase its temperature. In combination with the higher thermal conductivity and the lower dynamic viscosity, this means the convective heat transfer between storage medium and host-rock material with the surroundings will increase for hydrogen in comparison to natural gas (Nieland, 2008).

Conversely, the thermodynamic behaviour of hydrogen compared to natural gas is different when comparing the Joule-Thomson effect. Hydrogen inhibits a negative Joule-Thomson coefficient, which means it heats up during an isenthalpic pressure reduction, while natural gas cools down. Additionally, to this, the magnitude of the coefficient is much smaller than for natural gas, meaning the general influence of the Joule-Thomson effect is much smaller for hydrogen.

The interaction of these competing factors should be explored in a real-world in situ scenario, especially when applied to a fast-cycling operational profile.

8 Research gaps and recommendations for further investigations

The data discovery exercise undertaken for the Boulby Mine/evaporite succession has confirmed the knowledge on the local geology, and the geomechanical and thermodynamic properties of halite. However, significant unknowns exist for hydrogen with respect to how halite, and specifically the Boulby Halite, responds to fast cycling and associated changes of stress states. The following section provides a summary of the research gaps for the Boulby Halite, more generally for hydrogen storage in salt caverns, and the engineering and physical properties for storing hydrogen in the subsurface. These may be categorised into key themes: geomechanical responses, both locally and more generally for halite properties, thermodynamic responses to fast cycling, and the engineering challenges associated with hydrogen storage.

Geomechanical

- There is a need for cyclic creep tests, whereby mechanically applied loads and temperatures are changed. It is proposed to perform these tests uncoupled because currently cycling mechanical loads and temperatures simultaneously seems not to be advisable.
- The mechanism of internal damage due to cyclic temperature changes is not understood. This can be improved by large scale hollow cylinder tests, where temperature and pressure in the inner hole can be controlled independently from the applied stresses and temperature.
- Rock mechanical modelling for high frequency cycling of storage caverns in rock salt should be based on models coupling thermodynamics and rock mechanics. In doing so the interactive influence of the gas fill in the cavern and the rock mass can be considered.
- The conditions and parameters that influence cavern formation during solution mining may be further investigated, including grain size, alignment, insoluble material and stress state. These may be then linked to solution mining techniques to increase the time and resource efficiency of cavern construction.
- The permeability for open fractures and healed/annealing fractures should be investigated using laboratory measurements to better understand the risk of leakage from damaged cavern walls. Key questions regarding this include can over pressurisation of the cavern exceed the entry pressure for permeable flow.
- Investigation of the halite-non-halite interfaces as a potential point of failure during cycling operations. Understanding further how these interfaces may localised strain and reduce cavern stability and tightness. This may be tested for both general cavern control and specifically applied to the Boulby Halite-Billingham Anhydrite interface.

Response of the Boulby Halite

- Few creep tests have been performed on the local Boulby Halite at the Boulby Mine. Further detail on how the creep rate may change through the stratigraphy of the Boulby Halite would better constrain geomechanical models for cavern operation.
- The in-situ stress states for the Boulby Mine greatly impact the operational conditions for caverns within the Boulby Halite. Further constraining the deviatoric stress would constrain model parameters for future development.
- The thermal conductivity for the Boulby halite should be further constrained to refine boundary conditions for thermal modelling
- Investigation of the halite-non-halite interfaces as a potential point of failure during cycling operations. Understanding further how these interfaces may localised strain and reduce cavern stability and tightness. This may be tested for both general cavern control and specifically applied to the Boulby Halite-Billingham Anhydrite interface and also interbedded successions within the main evaporite units.

- A comparison of microscale laboratory tests to in situ field scale testing allowing for calibration of experimental laboratory data in real-world conditions.

Thermodynamic response

- Competing processes will influence the physical response of hydrogen-halite interface. Hydrogen has a negative Joule-Thompson affect, meaning that hydrogen will cool during compression. This will counteract the heating and thermal dissipation from the geothermal gradient. How these interact and influence the cavern stability for Boulby should be further investigated.

Engineering challenges

- The integrity at the casing shoe is of particular interest for cavern leakage. The well represents the point of highest leakage risk in the subsurface, and if high frequency cycling of pressure is planned then this may exasperate this weakness within the halite/cap rock. The suitability of material and the tightness of the interfaces between rock salt, cementation and casing should be studied in a laboratory test using large scale specimens.

9 Conclusion

Long duration energy storage methods, such as compressed air energy storage and hydrogen storage in salt caverns, will increasingly become a key component of a decarbonised and renewable-dominated electricity system. The subsurface geology of onshore NE England and the adjacent offshore region has the potential salt resource to contribute significantly to fulfilling the UK's future low carbon energy storage needs, with potential caverns providing capacity for storage in suitable areas. This is due to the underlying Southern Permian Basin and Zechstein Supergroup, which has been historically linked to hydrocarbon explorations and cavern storage but is recently the target for hydrogen storage investigations. The also area crucially hosts Boulby Mine which exploits a large halite and polyhalite deposits hosted within the Zechstein Supergroup. The Boulby Underground Laboratory (BUL), located at Boulby Mine, is a collaborative geophysical and physics laboratory that uses the subsurface conditions to investigate geo- and astro- physics. As part of the Secure Underground Caverns as an Energy Storage Solution (SUCcESS) project, BGS is establishing a geological research roadmap and as part of this, an understanding of what data exists for the geology at Boulby informed by literature review and data discovery exercise is a key resource. Topics for the review include the geomechanical properties of halite, the regional geological setting for the Southern Permian Basin, and local geology of Boulby. The findings from the data discovery exercise have highlighted key research topics that may be explored using the BUL facility.

Halite is widely viewed as an ideal host rock for man-made caverns due to its relative ease of construction by solution mining. Halite also holds favourable deformation characteristics granting for self-healing/annealing, low permeability and low reactivity, allowing for solution mined caverns to store liquid or gaseous products, including hydrogen or compressed air, in the subsurface for decades.

A wealth of understanding has been gathered across the western part of the southern Permian Basin in NE England and the Southern North Sea. The Boulby Mine is host to halite and polyhalite from the Zechstein Supergroup, a Permian succession of cyclical carbonate-evaporite which was deposited extensively in partially restricted marine conditions across NW Europe in the Southern and Northern Permian Basins. Episodic flooding and isolation of the basin led to the development of five major transgressive cycles, which in the UK are referred to as the (Zechstein) Z1 to Z5 cycles. Boulby Mine is located within the Z3 cycle and primarily targets the Boulby Potash. The potash is bounded by the Boulby Halite underneath, which is used as the mines main arterial roadway and is the main target of the SUCcESS study and succeeded by the Carnallitic Marl. Underlying the Boulby Halite is the Billingham Anhydrite. The Boulby Potash and Halite have been subject to mobilisation from chemical dissolution and precipitation,

and mechanical movements by thrust faulting, folding and halokinesis. The Boulby Halite consists of *c.* 50 m thick massive halite with subordinate mineral assemblages. Beneath the Boulby Halite are magnesium limestones, perhaps 200-300 m thick with minor Hayton Anhydrite and Kirkham Abbey Formation.

5 publicly accessible wells have been identified which intersect the Boulby Halite in the immediate vicinity of Boulby Mine, Staithes 1-3, Boulby Mine Shaft 1 and Boulby Watchman. A stratigraphy for the local and immediate area of Boulby and Boulby Mine have been constructed. Seismic reflection surveys were shot in the Boulby vicinity between 1981-86 by Shell during oil and gas exploration of the area. Of interest, seismic line (SY82-10V) was shot in 1982 directly above the Boulby facility. Geomechanical tests on samples at Boulby Mine were undertaken at various stratigraphic levels including the Boulby Halite and Billingham Anhydrite. These elucidate the tensile and compressional strength, angle of friction, cohesion, Norton's parameter and creep rate for the evaporites.

Geomechanical laboratory tests have also been undertaken in the wider literature with respect to fast cyclical hydrogen storage in salt caverns on samples from Mississippi, USA. Samples were found to exhibit little to no strain when cycling between tensional and compressional stress states, that halite was tight to hydrogen gas and that the main exploitative leakage may be from a breach in the well shell casing or an anomalous zone of insoluble material within the host rock. Together with geomechanical tests conducted on the Boulby Halite evidence that Boulby would be a suitable location for hydrogen storage and that cavern closure would be relatively slow if minimum pressures were not maintained.

The literature review for the suitability of salt for hydrogen storage and use of Boulby as a halite geo-physical laboratory has enlightened key research questions that are currently unknown or that require further investigation. Key research themes centre on geomechanical uncertainty and engineering responses, both for local Boulby Halite and wider salt cavern properties. Local investigations may include measuring the local creep rate, thermal conductivity, the deviatoric stress for placing caverns closer together, and responsiveness of the Boulby Halite to solution mining. Wider investigations may include the integrity at the casing shoe for cavern leakage, mechanism of internal damage due to cyclic temperature changes, impact of hydrogen-cooling during compression, and halite-non-halite interfaces as a potential point of failure during cycling.

Appendix 1

9.1 STAITHES 1 BOREHOLE

Tables A1-3 showing details for the Staithes 1 borehole, including well report, depth and formation tops.

Well name	STAITHES 1
Primary target	Conventional Oil and Gas
UKOGL ID	000669
NSTA Ref	L41/11- 2
BGS Ref	NZ71NE9
BGS SOBI Scan Link	620314
Operator	HOME
Spud Date	20 Sept 1965
Completion Date	06 Oct 1965
Coordinates (BNG)	476950, 518513 BGS Easting, Northing
Deviated	Vertical
Measured Depth Datum	Kelly Bushing
Datum Elevation	KB 222ft67.7m
Ground Level	210ft64.0m
TD	4975ft1516.4m
TVD SS	4753ft1448.7m
TD Age	Carboniferous
TD Formation Name	Carboniferous

UKOGL Well ID	000669	Operator	HOME
Spud Date	20 Sep 1965	Completed Date	06 Oct 1965
Surface Location (BNG)	X=476950 Y=518513	Deviated	No
Measured Depth Datum	Kelly Bushing	Original Depth Units	feet
Datum Elevation	222ft 67.7m	Ground Level	210ft 64.0m
Surface Formation	Lias	Surface Formation Age	Lower Jurassic

Formation Tops	**Age**	**MD (ft)**	**MD (m)**	**TVDSS (ft)**	**TVDSS (m)**
Penarth Group (Rhaetic)	Upper Triassic	882	268.8	660	201.2
Triassic Sandstone (Bunter)	Lower Triassic	1802	549.2	1580	481.6
Upper Magnesian Limestone	Upper Permian	3814	1162.5	3592	1094.8
Carboniferous Indeterminate	Carboniferous	4915	1498.0	4693	1430.4
TD (Carboniferous)	Carboniferous	4975	1516.4	4753	1448.7

9.2 GEOMECHANCIAL DATA FROM BOULBY

Unit	Sample	Deviatoric stress (MPa)	Strain rate (s^{-1})	n	A (T=40°C)
BH6/7	BH6/7-S4-CR	5	$4.40\ 10^{-11}$	1.53	$3.46\ 10^{-12}$
		10	$9.14\ 10^{-11}$		
		15	$2.50\ 10^{-10}$		
DHS	DHS-S16-CR1	5	$2.78\ 10^{-11}$	1.61	$2.23\ 10^{-12}$
		10	$1.11\ 10^{-10}$		
		15	$1.55\ 10^{-10}$		
	DHS-S36/42-CR2*	5	$1.10\ 10^{-10}$	4.06	$1.59\ 10^{-13}$
		10	$1.84\ 10^{-09}$		
BH9	BH9-S23-CR1	5	$5.90\ 10^{-11}$	1.37	$6.23\ 10^{-12}$
		10	$1.31\ 10^{-10}$		
		15	$2.74\ 10^{-10}$		
	BH9-S20-CR2	5	$3.47\ 10^{-11}$	2.08	$1.19\ 10^{-12}$
		10	$1.37\ 10^{-10}$		
		15	$3.47\ 10^{-10}$		
TRH	TRH-S50-CR1	5	$1.30\ 10^{-10}$	1.29	$1.45\ 10^{-11}$
		10	$2.05\ 10^{-10}$		
		15	$5.79\ 10^{-10}$		
	TRH-S52-CR2	5	$1.56\ 10^{-10}$	1.88	$6.96\ 10^{-12}$
		10	$4.22\ 10^{-10}$		
		15	$1.31\ 10^{-09}$		
* Sample broken during the third deviatoric stage, tertiary creep starts after around 55 days					

Table A4, Summary of geomechanical data from Hadj-Hassen 2021, determining the creep rate for the Boulby Halite. Strain rate in s^{-1} and deviatoric stress in MPa.

Table 16: Average properties of the Boulby project rocks

Parameter	Unit	Rock salts					Anhydrite	Comments
		POL	BH6/7	DHS	BH9	TRH	BMA	
Density	Kg/m^3	1984	2111	2171	2149	2144	2839	- Relatively low density for rock salts, except DHS - High density of anhydrite
Sound velocity	m/s	3411	2936	3498	3603	3616	5752	- Low sound velocity expresses the presence of fractures (stratification) and poor cementation
Tensile strength	MPa	1.24	0.84	1.42	1.91	1.97	5.71	- Relatively low tensile strengths for POL, BH6/7 and DHS - High tensile strength for anhydrite
Unconfined compression strength (UCS)	MPa	-	19.8	19.0	24.0	25.4	42.9	- Relatively low UCS for BH6/7 and DHS - UCS of anhydrite is expected to be higher (tested sample containing salt)
Young Modulus	GPa	-	-	10.5	21.7	28.2	55.4	- Low Young modulus of DHS (measurement affected by insoluble materials)
Poisson ratio	--	-	-	0.21	0.25	0.29	0.31	
Dilation Strength: average a-parameter b-parameter	MPa -- MPa	-	-	-	35 2.5 10.0	-	-	- Triaxial tests were conducted only for BH9 salt - The relation of the dilating deviatoric stress is given here versus the confining pressure
Cohesion	MPa	-	-	-	-	-	15.4	- The corresponding UCS is 59.1MPa
Friction angle	°	-	-	-	-	-	35	
Creep Index	%	-	0.27	0.23	0.32	0.66	-	- Average values of the 2 conducted tests - Broken sample of DHS is not considered

Table A5, Summary of geomechanical data from Hadj-Hassen 2021, providing overall geomechanical parameter averages for the Boulby Halite and Billingham Anhydrite.

Lithology	σ_v MPa	T °C	ε^s 1/d	n
BH6/BH7	5	40	5.00E-06	2.2
	10		4.00E-06	
	15		8.00E-06	
	20		1.90E-05	
POLYS	5	40	5.00E-06	4.1
	10		6.00E-06	
	15		2.00E-05	
	20		1.00E-04	

Table A6, Summary of geomechanical data from Claustal et al. 2021, determining the creep rate for the Boulby Halite.

Table 4.1	**Results of hydraulic fracturing tests in borehole PQ05** (P_{hyd}: hydrostatic pressure, P_c: breakdown-pressure, P_r: refrac-pressure, T: hydraulic tensile strength, P_{si}: shut-in pressure, θ: fracture strike direction (North over East), β: dip direction (North over East), α: dip (with respect to vertical)								
TVD [m]	P_c [MPa]	P_r [MPa]	T [MPa]	P_{si} [MPa]	frac trace	θ [deg]	β [deg]	α [deg]	remark
1106.5	-	15.9	-	16.6	A B	78 115	168 205	90 26	axial single trace subhorizontal frac.
1107.7	-	15.4 - 16.6 <16.0>[3]	-	16.7	no fractures detected				
1109.0	-	18.1	-	17.8	A B	62 178	152 268	76 43	steeply inclined frac. inclined fracture
1111.5	25.0	18.5	6.5	20.0	A B C	54 170 65	324 260 155	56 50 69	inclined fracture inclined fracture steeply inclined frac.
1115.5	-	21.2	-	23.0	A	177	87	90	axial single trace
1120.0	-	21.6 - 22.3 <21.95>	-	26.4	A B C	39 168 32	309 78 122	90 90 22	axial single trace axial single trace subhorizontal frac.
1125.0	-	21.9 - 23.5 <22.7>	-	28.0	A B	3 45	93 315	90 90	axial single trace axial single trace
1129.0	30.8	23.9	6.9	25.4	A	66	336	84	steeply inclined frac.
1134.0	-	23.0 - 25.1 <24.05>	-	26.5[4]	A	144	234	22	subhorizontal frac.
1141.0	-	22.5 - 25.0 <23.75>	-	30.2[5]	A B	115 146	205 236	90 90	axial single trace axial double trace

Table A7. A summary of Solexperts GmbH (2021) geomechanical hydraulic fracturing measurements from the Boulby Halite on borehole PQ05.

.

References

Ahluwalia, R.K., Hua, T.Q., Peng, J.K. and Kumar, R., 2019, April. System level analysis of hydrogen storage options. In *US DOE Hydrogen and Fuel Cells Program 2019 Annual Merit Review and Peer Evaluation Meeting*.

Allen, K., 1972. Eminence dome-natural-gas storage in salt comes of age. *Journal of Petroleum Technology*, *24*(11), pp.1299-1301. https://doi.org/10.2118/3433-PA

Allsop, C., Yfantis, G., Passaris, E. and Edlmann, K. 2023. Utilizing publicly available datasets for identifying offshore salt strata and developing salt caverns for hydrogen storag. *Geological Society of London.* https://doi.org/10.6084/m9.figshare.c.6315742.

Barnett, H.G., Ireland, M.T. and Van Der Land, C., 2024. Capturing Geological Uncertainty in Salt Cavern Developments for Hydrogen Storage. *Earth Science, Systems and Society*, *4*, p.10125. https://doi.org/10.3389/esss.2024.10125

Bérest, P., 2019. Heat transfer in salt caverns. *International Journal of Rock Mechanics and Mining Sciences*, *120*, pp.82-95. https://doi.org/10.1016/j.ijrmms.2019.06.009

Bérest, P., Brouard, B., Hévin, G. and Réveillère, A., 2021, June. Tightness of salt caverns used for hydrogen storage. In *ARMA US Rock Mechanics/Geomechanics Symposium* (pp. ARMA-2021). ARMA.

Beutel, T. and Black, S.T., 2005. Salt deposits and gas cavern storage in the UK with a case study of salt exploration from Cheshire. Erdoel Erdgas Kohle, 121. https://www.osti.gov/etdeweb/biblio/20589691

BGS Core Scanning Facility. (2024). Boulby Watchman borehole, core scanning dataset. NERC EDS National Geoscience Data Centre. (Dataset). https://doi.org/10.5285/99a70d6a-b767-4484-8b73-7a5ee2e2f68f

Brackenridge, R.E., Underhill, J.R., Jamieson, R. and Bell, A. 2020. Structural and stratigraphic evolution of the Mid North Sea High region of the UK Continental Shelf. Petroleum Geoscience, 26, 154–173, https://doi.org/10.1144/petgeo2019-076.

Buchholz, S. and Keffeler E. Dusterloh 2023. Determination of Thermal Expansion Coefficient of Damaged Rock Salt Under Unconfined Conditions to Address Thermally Induced Stresses in Cyclic Storage Caverns. SMRI Research Report RR2022-3, prepared by RESPEC, Rapid City, SD, United States, and Clausthal University of Technology, Clausthal-Zellerfield, Germany, for the *Solution Mining Research Institute*.

Buchholz, S., E. Keffeler, and U. Düsterloh, 2020. Determination of Thermal Expansion Coefficient by Stress-Controlled and Volume-Controlled Triaxial Tests to Address Thermal-Induced Stresses in Cyclic Storage Caverns, SMRI Research Report RR2020-2, prepared by RESPEC, Rapid City, SD, United States, and Clausthal University of Technology, Clausthal-Zellerfield, Germany, for the *Solution Mining Research Institute*, Clifton Park, NY, United States.

Caglayan, D.G., Weber, N., Heinrichs, H.U., Linßen, J., Robinius, M., Kukla, P.A. and Stolten, D. 2020. Technical potential of salt caverns for hydrogen storage in Europe. International Journal of Hydrogen Energy, 45, 6793–6805, https://doi.org/10.1016/j.ijhydene.2019.12.161.

Cameron, T. D. J., Crosby, A., Balson, P. S., Jeffery, D. H., Lott, G. K., Bulat, J., And Harrison, D. J., 1992. United Kingdom offshore regional report: the geology of the southern North Sea. London, HMSO for the British Geological Survey.

Cárdenas, B., Swinfen-styles, L., Rouse, J. and Garvey, S.D. 2021b. Short-, medium-, and long-duration energy storage in a 100% renewable electricity grid: A UK case study. Energies, 14, https://doi.org/10.3390/en14248524.

Cárdenas, B., Swinfen-Styles, L., Rouse, J., Hoskin, A., Xu, W. and Garvey, S.D. 2021a. Energy storage capacity vs. renewable penetration: A study for the UK. Renewable Energy, 171, 849–867, https://doi.org/10.1016/j.renene.2021.02.149.

Chen, Y., Jin, X., Zeng, L., Zhong, Z., Mehana, M., Xiao, W., Pu, W., Regenauer-Lieb, K. and Xie, Q., 2023. Role of large-scale underground hydrogen storage and its pathways to achieve net-zero in China. Journal of Energy Storage, 72, p.108448. https://doi.org/10.1016/j.est.2023.108448

Daniels, K.A., Harrington, J.F., Wiseall, A.C., Shoemark-Banks, E., Hough, E., Wallis, H.C. and Paling, S.M. 2023. Battery Earth: using the subsurface at Boulby underground laboratory to investigate energy storage technologies. Frontiers in Physics, 11, https://doi.org/10.3389/fphy.2023.1249458.

Davison, I. 2009. Faulting and fluid flow through salt. Journal of the Geological Society, 166, 205–216, https://doi.org/10.1144/0016-76492008-064.

Evans, D.J. and Holloway, S. 2009. A review of onshore UK salt deposits and their potential for underground gas storage. Geological Society Special Publication, 313, 39–80, https://doi.org/10.1144/SP313.5.

Field, L.P., Milodowski, A.E., Evans, D., Palumbo-Roe, B., Hall, M.R., Marriott, A.L., Barlow, T. and Devez, A., 2019. Determining constraints imposed by salt fabrics on the morphology of solution-mined energy storage cavities, through dissolution experiments using brine and seawater in halite. *Quarterly Journal of Engineering Geology and Hydrogeology*, 52(2), pp.240-254. https://doi.org/10.1144/qjegh2018-072

Fyfe, L.J. And Underhill, J.R. 2023a. The Upper Permian Zechstein Supergroup Of NE England And The Adjacent Southern North Sea: A Review Of Its Role In The Uk's Energy Transition. Journal Of Petroleum Geology, 46, 383–406, Https://Doi.Org/10.1111/Jpg.12843.

Fyfe, L.J.C. And Underhill, J.R. 2023b. A Regional Geological Overview Of The Upper Permian Zechstein Supergroup (Z1 To Z3) In The SW Margin Of The Southern North Sea And Onshore Eastern England. Journal Of Petroleum Geology, 46, 223–256, Https://Doi.Org/10.1111/Jpg.12837.

Fyfe, L.J.C., Schofield, N., Holford, S.P., Heafford, A. and Raine, R. 2020. Geology and petroleum prospectivity of the Larne and Portpatrick basins, North Channel, offshore SW Scotland and Northern Ireland. Petroleum Geoscience, 26, 272–302, https://doi.org/10.1144/petgeo2019-134.

Grant, R.J., Underhill, J.R., Hernández-Casado, J., Barker, S.M. and Jamieson, R.J. 2019. Upper Permian Zechstein Supergroup carbonate-evaporite platform palaeomorphology in the UK Southern North Sea. Marine and Petroleum Geology, 100, 484–518, https://doi.org/10.1016/j.marpetgeo.2017.11.029.

Gschnitzer, E., Wenger, J. and Raine, A. 2020. Woodsmith project – Construction of a 37 km long mineral transport system for the world's largest Polyhalite resource. Geomechanik und Tunnelbau, 13, 643–649, https://doi.org/10.1002/geot.202000019.

Handford, C.R. 1991. Marginal marine halite: sabkhas and Salinas. In: Melvin, J.L. (ed), Evaporites, petroleum and mineral resources. Elsevier Developments in Sedimentology, 50, 1-66. https://doi.org/10.1016/S0070-4571(08)70259-0

Hansen, F.D., Kuhlman, K.L. and Sobolik, S. 2016. Considerations of the Differences between Bedded and Domal Salt Pertaining to Disposal of Heat-Generating Nuclear Waste. Report to US DoE, Used Fuel Disposition Campaign, Sandia National Laboratories, July 7, 2016 FCRD-UFRD-2016-000441, SAND2016-6522R, 55 pp. https://doi.org/10.2172/1333710

IDRIC, 2024, Assessing the Regional Demand for Geological Hydrogen Storage: Building a Strategic Case for Investment in the East Coast Cluster. Industrial Decarbonisation Research and Innovation Centre, Edinburgh.

IDRIC. Mar 2022. Cluster Mapping Report: The Humber industrial cluster.

IEA Hydrogen Technology Collaboration Program, 2022. 2022 Annual Report: Tasks & Member Updates. Available online: https://www.ieahydrogen.org/annual-reports/ . Accessed on November 2023.

James, B.D., Houchins, C., Huya-Kouadio, J.M. and Desantis, D.A. 2016. Final Report: Hydrogen Storage System Cost Analysis Sponsorship and Acknowledgements.

Johnson, H., Warrington, G. And Stoker, S. J., 1994. Permian And Triassic Of The Southern North Sea. In: Knox, R. W. O'b. And Cordey, W. G. (Eds), Lithostratigraphic Nomenclature Of The Uk North Sea. British Geological Survey, Nottingham.

Kaldemeyer, C., Boysen, C. and Tuschy, I., 2016. Compressed air energy storage in the German energy system–status quo & perspectives. Energy Procedia, 99, pp.298-313. https://doi.org/10.1016/j.egypro.2016.10.120

Kemp, S.J., Smith, F.W., Wagner, D., Mounteney, I., Bell, C.P., Milne, C.J., Gowing, C.J.B. and Pottas, T.L., 2016. An improved approach to characterize potash-bearing evaporite deposits, evidenced in North Yorkshire, United Kingdom. *Economic Geology*, *111*(3), pp.719-742. https://doi.org/10.2113/econgeo.111.3.719

Khan, M.A.I., Piñerez Torrijos, I.D., Algazban, S.H.A., Strand, S. and Puntervold, T., 2022, October. Polysulphate: A New EOR Additive to Maximize the Oil Recovery from Carbonate Reservoirs at High Temperature. In Abu Dhabi International Petroleum Exhibition and Conference (p. D041S114R004). SPE. https://doi.org/10.2118/211443-MS

Kondziella, H., Specht, K., Lerch, P., Scheller, F. and Bruckner, T., 2023. The techno-economic potential of large-scale hydrogen storage in Germany for a climate-neutral energy system. Renewable and Sustainable Energy Reviews, 182, p.113430. https://doi.org/10.1016/j.rser.2023.113430

Kotarba, M.J., Peryt, T.M., Kosakowski, P. and Wiecław, D. 2006. Organic geochemistry, depositional history and hydrocarbon generation modelling of the Upper Permian Kupferschiefer and Zechstein Limestone strata in south-west Poland. Marine and Petroleum Geology, 23, 371–386, https://doi.org/10.1016/j.marpetgeo.2005.10.003.

Lee, J., 2022. Faults, fractures and fluids in mudstones during Cenozoic extension in the Cleveland Basin (Doctoral dissertation, Durham University).

Lincoln, P.C., Eddey, L., Matthews, I., Palmer, A. and Bateman, M., 2017. The Quaternary of the Vale of Pickering QRA Field Guide.

Liu, W., Li, Q., Yang, C., Shi, X., Wan, J., Jurado, M.J., Li, Y., Jiang, D., Chen, J., Qiao, W. and Zhang, X., 2023. The role of underground salt caverns for large-scale energy storage: A review and prospects. *Energy Storage Materials*, p.103045. https://doi.org/10.1016/j.ensm.2023.103045

Lord, A.S., Kobos, P.H. and Borns, D.J. 2014. Geologic storage of hydrogen: Scaling up to meet city transportation demands. International Journal of Hydrogen Energy, 39, 15570–15582, https://doi.org/10.1016/j.ijhydene.

Louvet, F., Y. Charnavel, and G. Hevin. 2017. 'Thermodynamic studies of hydrogen storage in salt caverns', SMRI Spring.

Manning, P. I. And Wilson, H. E. 1975. The Stratigraphy of the Larne Borehole, Co. Antrim. Bull. Geol. Surv. G.B. 50, 1-50.

Marschall, P., Horseman, S. and Gimmi, T., 2005. Characterisation of gas transport properties of the Opalinus Clay, a potential host rock formation for radioactive waste disposal. *Oil & gas science and technology*, *60*(1), pp.121-139. https://doi.org/10.2516/ogst:2005008

Mellegard, K. and U. Düsterloh, 2012. High Frequency Cavern Cycling – Phase 2: Cyclical Loading Effects on the Dilation and Creep Properties of Salt, SMRI Research Report RR2012-2, prepared by RESPEC, Rapid City, SD, United States, and Clausthal University of Technology, Clausthal-Zellerfield, Germany, for Solution Mining Research Institute, Clarks Summit, PA, United States.

Mellegard, K. D., 2013. High Frequency Cavern Cycling—Phase 2-B: Extensional Cyclic Fatigue Testing of Salt, SMRI Research Report RR2013-2, prepared by RESPEC, Rapid City, SD, for Solution Mining Research Institute, Clarks Summit, PA.

Minas, Sophie, and Nils Skaug. 2021. 'Hydrogen Salt Cavern Design', SMRI Fall 2021 Technical

Miocic, J., Heinemann, N., Edlmann, K., Scafidi, J., Molaei, F. and Alcalde, J. 2023. Underground hydrogen storage: a review. Geological Society, London, Special Publications, 528, 73–86, https://doi.org/10.1144/sp528-2022-88.

National Grid ESO. Data Portal. Accessed Feb 2024. https://www.nationalgrideso.com/data-portal

Nieland, J. D. 2008. "Salt cavern thermodynamics–comparison between hydrogen, natural gas, and air
NWS. 2018. UK Halite Deposits - Structure, Stratigraphy, Properties and Post-closure Performance

Parkes, D., Evans, D.J., Williamson, P. and Williams, J.D.O., 2018. Estimating available salt volume for potential CAES development: A case study using the Northwich Halite of the Cheshire Basin. Journal of Energy Storage, 18, pp.50-61. https://doi.org/10.1016/j.est.2018.04.019

Passaris, E.K.S. and Noden, R. 2011. Geomechanical parametric studies for a propane storage cavern in North Tees saltfield in the UK. Solution Mining Research Institute (SMRI) Fall 2011 Technical Conference York, United Kingdom, 3–4 October 2011, 10 pp.

Penn, I.E., Holliday, D.W., et al. 1983. The Larne No. 2 Borehole: discovery of a new Permian volcanic centre. Scottish Journal of Geology, 19, 333–346. https://doi.org/10.1144/sjg19030333

Peryt, T. M., Geluk, M. C., Mathiesen, A., Paul, J. And Smith, K., 2010. Zechstein. In: Doornenbal, J.C. and Stevenson, A.G. (Eds), Petroleum Geological Atlas of the Southern Permian Basin Area. EAGE, Houten, The Netherlands, 123-147.

Roberts, N.M.W., Lee, J.K., Holdsworth, R.E., Jeans, C., Farrant, A.R. and Haslam, R. 2020. Near-surface Palaeocene fluid flow, mineralisation and faulting at Flamborough Head, UK: New field observations and U-Pb calcite dating constraints. Solid Earth, 11, 1931–1945, https://doi.org/10.5194/se-11-1931-2020.

Schlichtenmayer, M., A. Bannach, M. Amro, and C. Freese. 2015. 'Renewable Energy Storage in Salt Caverns-Comparison of Thermodynamics and Permeability between Natural Gas, Air and Hydrogen', SMRI research report RR2015-1.

Smith, D.B., 1989. The late Permian palaeogeography of north-east England. *Proceedings of the Yorkshire Geological Society*, *47*(4), pp.285-312. https://doi.org/10.1144/pygs.47.4.285

Smith, D.B., 1996. Deformation in the late Permian Boulby Halite (EZ3Na) in Teesside, NE England. *Geological Society, London, Special Publications*, *100*(1), pp.77-87.

Swift, G.M. and Reddish, D.J., 2005. Underground excavations in rock salt. *Geotechnical & Geological Engineering*, *23*, pp.17-42. https://doi.org/10.1144/GSL.SP.1996.100.01.07

Talbot, C., Tully, C. and Woods, P. 1982. The Structural Geology Of Boulby (Potash) Mine, Cleveland, United Kingdom. Tectonophysics, 85, 167–204. https://doi.org/10.1016/0040-1951(82)90102-0

Tarkowski, R. 2019. Underground hydrogen storage: Characteristics and prospects. Renewable and Sustainable Energy Reviews, 105, 86–94, https://doi.org/10.1016/j.rser.2019.01.051.

Tarkowski, R., Lankof, L., Luboń, K. and Michalski, J., 2024. Hydrogen storage capacity of salt caverns and deep aquifers versus demand for hydrogen storage: A case study of Poland. Applied Energy, 355, p.122268. https://doi.org/10.1016/j.apenergy.2023.122268

Tees Valley Combined Authority. Mar 2023. Net Zero Strategy for Tees Valley.

The Royal Society. 2023. Large-scale electricity storage.

Tucker, M.E. 1991. Sequence stratigraphy of carbonate-evaporite basins: models and application to the Upper Permian (Zechstein) of northeast England and adjoining North Sea. Journal of the Geological Society, 148, 1019–1036. https://doi.org/10.1144/gsjgs.148.6.1019

Turner, P. and Magaritz, M. 1986. Chemical and isotopic studies of a core of Marl Slate from NE England: influence of freshwater influx into the Zechstein Sea. Geological Society Special Publication, 22, 19–29. https://doi.org/10.1144/GSL.SP.1986.022.01.03

UKRI 2022. Tees Valley Net Zero.

Underhill, J.R. and Hunter, K.L. 2008. Effect of Zechstein Supergroup (Z1 cycle) Werrahalit pods on prospectivity in the southern North Sea. American Association of Petroleum Geologists Bulletin, 92, 827–851, https://doi.org/10.1306/02270807064.

Underhill, J.R., De Jonge-Anderson, I., Hollinsworth, A.D. and Fyfe, L.C. 2023. Use of exploration methods to repurpose and extend the life of a super basin as a carbon storage hub for the energy transition. AAPG Bulletin, 107, 1419–1474, https://doi.org/10.1306/04042322097.

Van Gessel, S.F., Groenenberg, R.M., Juez-Larré, J. and Dalman, R.A.F., 2022. Underground hydrogen storage in salt caverns in the Netherlands–Storage performance and implications for geomechanical stability. In The Mechanical Behavior of Salt (pp. 607-615).

Warren, J.K. 2006. Evaporites: Sediments, Resources and Hydrocarbons. Berlin, Springer, 1036 pp. https://doi.org/10.1007/3-540-32344-9

White, M., Wilmont, R. 2018. UK Halite Deposits – Structure, Stratigraphy, Properties and Post-closure Performance. *Galson Sciences Report to RWM*, 1735-1 v3. Galson Sciences, Oakham, UK.

Williams, J.D.O., Williamson, J.P., et al. 2022. Does the United Kingdom have sufficient geological storage capacity to support a hydrogen economy? Estimating the salt cavern storage potential of bedded halite formations. Journal of Energy Storage, 53, https://doi.org/10.1016/j.est.2022.105109.

Wilson 2023. Great Britain's energy daily data. Accessed Feb 2024. https://public.tableau.com/app/profile/grant.wilson/viz/GreatBritainsenergydailydata/GBenergyperday?publish=yes

Woods, P.J.E. 1979. The Geology of Boulby Mine. Economic Geology, 74, 409–418. https://doi.org/10.2113/gsecongeo.74.2.409

Wrighton, C E And Bide, T P. 2011. Mineral Safeguarding Areas for North Yorkshire County Council. British Geological Survey Commissioned Report, CR/11/132. 48pp.

Wrighton, C E, Bide, T P, Parry, S, And Linley, K A. 2013. Mineral Safeguarding Areas for North York Moors National Park Authority. British Geological Survey Commissioned Report, CR/13/073. 51pp.